Viability of spent coffee ground biochar as a filtration media to remove organic contaminants from urban stormwater in the Pacific Northwest

Nicole Redden

A thesis
Submitted in partial fulfillment of the
Requirements for the degree of

Master of Science in Civil Engineering

University of Washington
2021

Committee:
Jessica Ray (Committee Chair)
Edward Kolodziej

Program authorized to offer degree:
Civil and Environmental Engineering
University of Washington

Abstract

Viability of spent coffee grounds biochar as a filtration media to remove organic contaminants from urban stormwater in the Pacific Northwest

Rainfall on urban landscapes in densely populated cities can have severe impacts on the hydrologic cycle. Higher volumes of "urban stormwater" runoff can overwhelm stormwater management systems resulting in overflow events where runoff and/or raw sewage are directly discharged to receiving water bodies. Furthermore, urban stormwater contacts engineered and impervious surfaces (e.g., pavement, buildings, vehicles) during conveyance, transporting elevated concentrations of pollutants which threaten human and environmental health. Decentralized approaches known as best management practices (BMPs) are a potential solution to facilitate local groundwater recharge via stormwater infiltration, and to better manage large volumes of urban runoff to prevent overflow events; however, these systems are unable to adequately remove all contaminants present in urban runoff. This study analyzes biochar, a pyrolyzed biomass feedstock adsorbent, produced from spent coffee grounds (SCG) as a possible BMP amendment to treat stormwater contaminants during infiltration. Caffeine, atrazine, diuron, fipronil, and pentachlorophenol compounds were used as representative trace organics found in urban stormwater and exhibit a range of hydrophobicity. Organic compound adsorption capacities and rates on inactivated biochar (SCG 400) and potassium hydroxide (KOH) activated biochar (SCG KOH) were compared through surface characterization (e.g., fixed carbon content, porosity, and surface area) and batch sorption tests in a complex, simulated urban stormwater matrix. SCG KOH showed significant Brunauer-Emmett-Teller (BET) surface area increase over the SCG 400 precursor (852.11 m^2/g versus 2.66 m^2/g). Both SCG 400 and SCG KOH exhibited high fixed carbon contents (71.1% and 84.8% respectively) when compared to the SCG feedstock (17%). Batch tests indicated lower removal rates by SCG 400 when multi-pollutant contaminant mixtures or natural organic matter were introduced; yet, higher removal rates were observed in the simulated stormwater matrix. The higher rates are likely due to electron bridging effects. SCG KOH removed nearly all contaminants regardless of batch sorption conditions. Isotherm batch sorption tests for SCG KOH were inconclusive as the activated biochar removed even the highest concentrations (10,000 µg/L). Equilibrium adsorption was achieved within 1-12 hours in multi pollutant systems with no trend of preferential removal for more hydrophobic compounds. Bench scale column studies amended with 0 wt% (sand only), 0.5 wt%, and 3 wt% biochar showed long lifetimes and high removal capacities of SCG KOH with increased weight percent. For example, complete breakthrough for sand only columns occurred within 13 pore volumes (1.2 L), while the 3 wt% columns maintained complete removal of all contaminants until receiving 150 pore volumes (16 L) of heavily contaminated stormwater. Complete breakthrough of the 3 wt% columns has not been observed after 1200 pore volumes (130 L). The results of our study indicate that SCG biochar activated with KOH has a high adsorption rate for a wide variety of trace organic contaminants over a long lifetime. Additionally, while this study is focused on applications of biochar amendments to address urban stormwater pollution in the Puget Sound (Pacific Northwest), our approach is applicable worldwide.

Acknowledgements

First and foremost, I would express the deepest appreciation to my advisor and committee chair, Dr. Jessica Ray for both granting me this opportunity and supporting me thorough my research. Without Dr. Ray's patience, enthusiasm, and depth of knowledge this thesis would not have been possible. I would also like to thank my committee member, Dr. Edward Kolodziej for evaluating my thesis and providing expert feedback on my research.

Thank you to the Washington Research Foundation and UW CoMotion for seeing the potential of my project and supporting this research.

Additionally, I am incredibly grateful for the efforts and collaborations from my fellow lab members. Their feedback and revisions to my thesis, check-ins through "rose and thorn" conversations, and insightful discussions in our anti-racism book club improved my grad school experience tenfold even while living through a pandemic. Special acknowledgements go to Fanny, Jess S., and Joshua who ran all 600+ of my samples, provided invaluable insights into my data, and assisted with in-lab work.

Finally, I would like to thank my family and friends for constantly supporting me as I reach for my goals, even when it means moving 2,000 miles across the country. I love you all dearly.

Table of Contents

List of Figures

List of Tables

1. Introduction

As urbanization increases, natural land cover is converted to impermeable surfaces such as rooftops and pavement (Hogan and Walbridge 2007). This shift in land cover causes significant alterations to the hydrologic cycle. Impervious surface coverage decreases stormwater infiltration rates, reducing groundwater recharge and consequently diminishing an essential drinking and agricultural water source within the urban water supply (Berndtsson 2010, CWP 2003). Additionally, slower infiltration rates yield large volumes of stormwater runoff from streets and buildings known as "urban stormwater" (USGS 2021). Urban stormwater travels quickly over unclean, engineered surfaces, which often overwhelms storm drains and receiving water bodies causing street flooding, increased erosion, and aquatic habitat damage (McGrane 2016). In the Pacific Northwest, one acre of impervious land cover results in nearly five times the volume of runoff when compared to natural land cover (**Figure 1.1)** (King County 2020).

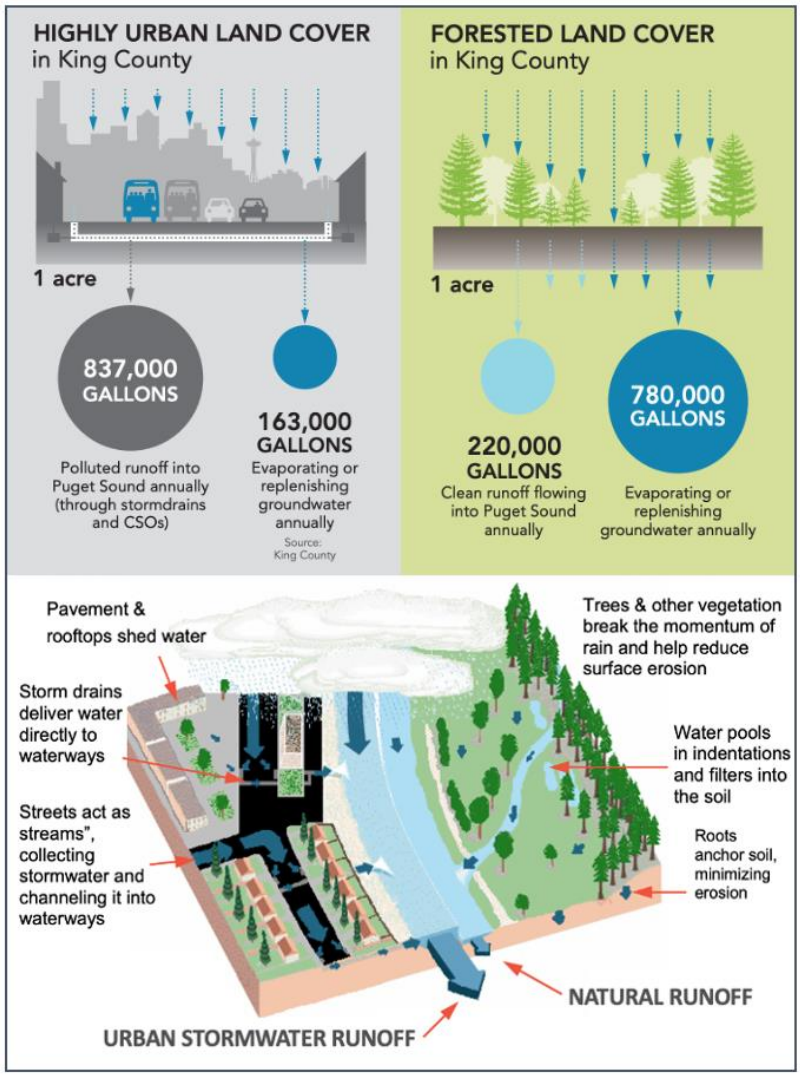

Figure 1.1 (Top) Illustration comparing differences in groundwater recharge from stormwater runoff within urbanized (left) and natural (right) land cover in the Puget Sound Region (King County 2020). **(Bottom)** Additionally, this figure depicts the increase in runoff from impervious surface coverage compared to open forested land (adapted from Knudson and Vogel 2005)

These effects from increased impervious land cover are expected to worsen as worldwide populations are growing and living in more urban landscapes (Exum et al., 2005). The Puget Sound region in particular is one of the most rapidly urbanizing areas in the country: the population is predicted to grow by 10% (from 5.2 to 5.7 million) in the next 10 years (TNC 2021). This explosive growth will have severe consequences for stormwater runoff as more natural land is eliminated to make way for housing and urbanization.

In addition to urbanization, climate change affects the volume of stormwater runoff by varying the frequency and intensity of extreme weather events including both precipitation and droughts (Sharma et al. 2016). Cities like Seattle, Washington, that already experience frequent rain events are expected to have storms of heightened intensity resulting in increased urban stormwater runoff volume. King County, Seattle's most populous county, has proposed investing $88.4 million in combined sewer overflow reduction and green stormwater infrastructure in the 2021-2022 budget to decrease runoff volume within the county (King County 2020). In contrast, other cities that struggle to meet the water demand are receiving lower amounts of precipitation and have started exploring urban stormwater as a water resource to augment the water supply. For example, Los Angeles, California voted to approve a $500 million program to implement projects that retain and reuse or treat stormwater onsite (Hagekhalil et al. 2014). The imbalance of water and the consequences of climate change are predicted to worsen as urbanization and population increase exacerbates climate change. As such, urban stormwater has become an increasingly important component of the urban hydrologic cycle.

1.1 Stormwater Pollution

Urban stormwater is one of the largest nonpoint sources of pollution in surface waters (Lee and Bang 2000, Milesian 2015, Chow 2019). Precipitation falls on urban, engineered surfaces such as roads, metal pipes, and concrete, contacting and transporting contaminants as it flows to storm drains and nearby water bodies. Expanding impervious surfaces associated with urbanization increases the variety and concentration of pollutants in stormwater runoff (**Table 1.1**). Some examples of prevalent contaminants include oils, grease, and toxic chemicals from motor vehicles, dissolved heavy metals such as zinc, lead, and copper from metal pipes and motor vehicles, and pesticides from lawns and gardens (Göbel, Dierkes, and Coldewey 2007, Zgheib, Moilleron, and Chebbo 2012). Additionally, high precipitation events can lead to sewer overflows posing a risk of contamination from hydrophobic organic pollutants, volatile organic compounds, nutrients, biological oxygen demand, and antibiotic resistant pathogens (Gasperi, Laborie, and Rocher 2012). Chronic and acute illnesses in humans have been linked to urban stormwater as humans are exposed through drinking water, seafood, and direct contact (Gaffield et al. 2003). For example, stormwater runoff is associated with elevated concentrations of microorganisms such as bacteria, *Giardia*, and *Cryptosporidium* and can lead to fecal coliform bacteria in surface waters at levels above the standards for recreation (Gaffield et al. 2003). **Table 1.1** summarizes national stormwater parameters and contaminant concentrations from the National Stormwater Quality Database by Pitt et al. as reported by Okaikue-Woodi et al. (Pitt et al. 2018), Okaikue-Woodi et al. 2020).

.

Table 1.1 Common categorizations, sources, and concentrations of urban stormwater constituents (Okaikue-Woodi et al. 2020).

Category	Constituent	Value	Unit
Physicochemical Parameters	TSS	133 ± 260	mg/L
	Oils and grease	10.0 ± 1.0	
	TKN	2.00 ± 3.5	
	NO2- and NO3-	0.900 ± 1.3	
	Total P	2.00 ± 3.50	
Heavy Metals	Zn	160 ± 356	μg/L
	Cu	26.5 ± 54.6	
	Pb	24.4 ± 60.6	
	Ni	7.20 ± 14.7	
	Cr	7.10 ± 13.5	
	Cd	1.50 ± 5.5	
Biological	Fecal coliforms	55151 ± 282910	#/100 mL
Trace Organic Compounds	benzene	84.7 ± 79.3	μg/L
	2-chloroethylvinylether	3.40 ± 2.60	
	chloroform	74.8 ± 160	
	dichlorobromoethane	0.800 ± 0.50	
	1,1-dichloroethane	0.600 ± 0.10	
	1,2-dichloroethane	1.50 ± 3.6	
	methylchloride	5.20 ± 4.1	
	methylenechloride	12.2 ± 9.4	
	tetrachloroethylene	1.50 ± 1.0	
	toluene	1.50 ± 2.1	
	1,1,1-trichloroethane	2.40 ± 2.0	

Calls for better stormwater management have grown in Seattle as stormwater runoff has been determined to degrade the health of salmon and salmon runs Salmon have particular significance in the Pacific Northwest as they are: (1) paramount to the identity and traditional practices of indigenous populations; (2) essential for commercial and recreational fishing; and (3) provide nutrients vital to the health and productivity of freshwater ecosystems (Feist et al. 2017). A variety of Pacific salmon, Coho salmon, are particularly susceptible to pollutants in stormwater, reporting up to 40-90% loss rates in urban streams before spawning (Tian et al. 2021). A recent study from researchers at the University of Washington discovered a direct link between a tire rubber antioxidant (6PPD-quinone) and Coho salmon pre-spawn mortality from stormwater runoff (Tian et al. 2021). The adverse ecological and human health impacts from urban stormwater pollution have led municipalities locally and worldwide to seek to upgrade their stormwater management systems.

1.2 Existing Stormwater Management Systems

The United States employs either sanitary or combined sewer system underground piping networks to convey stormwater from impervious surfaces to surface waters. Sanitary sewer systems (SSSs) separate sewage and industrial wastewater from stormwater, transporting sewage and industrial effluent to wastewater treatment plants and directly discharging urban stormwater to a nearby water body (**Figure 1.2**). Combined sewer systems (CSSs) are less common and usually found only in less recently developed areas such as downtown Seattle (ECOSS 2019). These sewer systems collect and convey urban stormwater, domestic sewage, and industrial discharge to a wastewater treatment plant before the effluent is discharged to a water body (**Figure 1.2**). During heavy precipitation, however, stormwater may exceed CSS or wastewater treatment plant capacity resulting in overflows and direct discharge of untreated human and industrial waste as well as other toxic materials and debris. Both CSSs and SSSs convey stormwater to a centralized location and allow for the discharge of stormwater contaminants to water bodies. While sanitary sewer systems are more common, serving almost 4 times the population of CSSs, CSSs lead to at least 85 times the amount of overflow discharge (**Figure 1.2**).

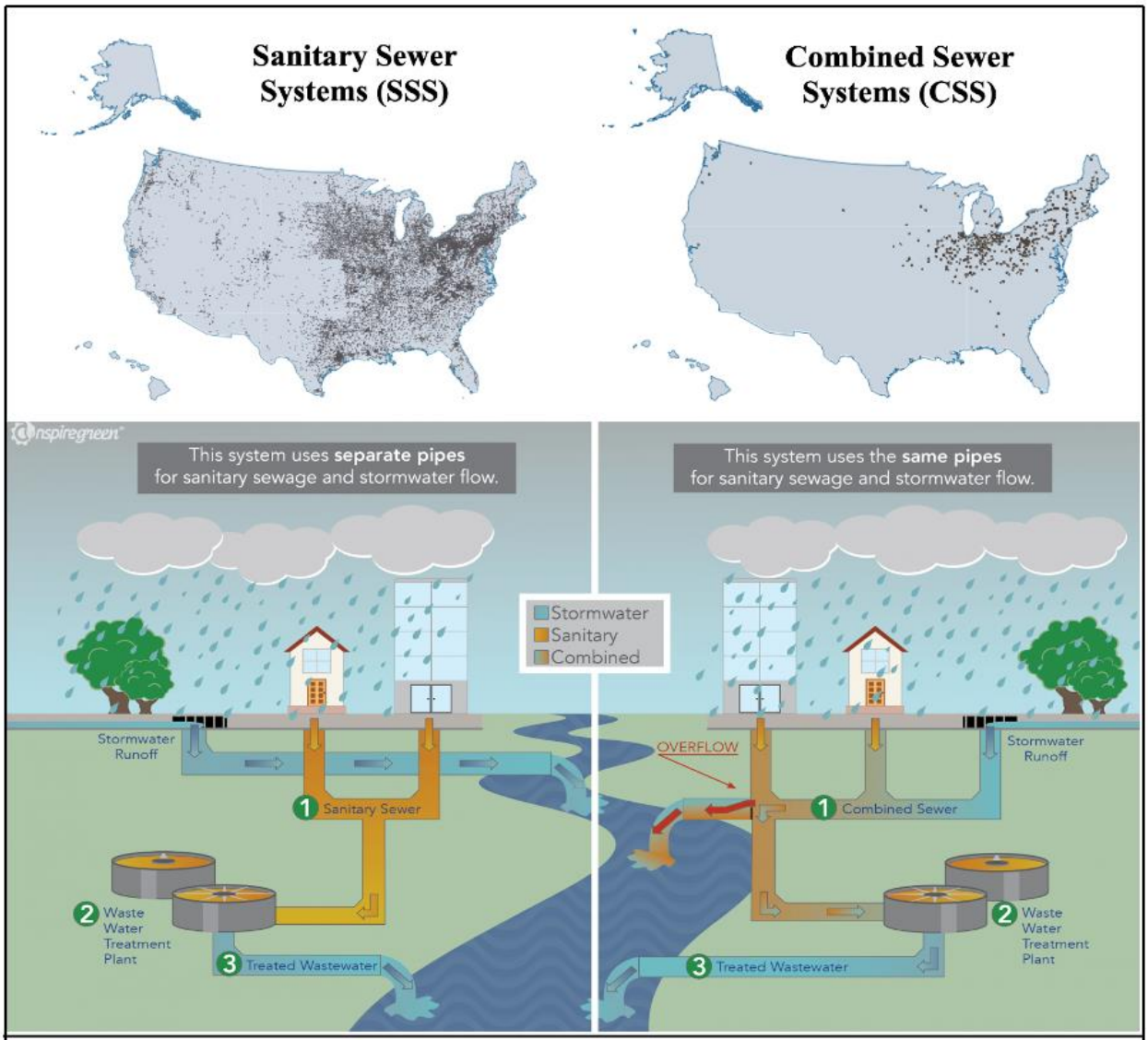

System Type	Number of Systems	Population Served	Estimated Annual Overflow Events	Overflow Volume Discharge
Combined Sewer (CSS)	1,100	43 million	43,000 - 60,000	850 billion gall
Sanitary Sewer (SSS)	20,428	164 million	23,000 - 75,000	3-10 billion gallons

Figure 1.2 Figure depicting the locations within the United States and flow paths of sanitary sewer systems (left) and combined sewer systems (right). Additionally, this figure reports the prevalence and overflow data for each type of system. (Nspiregreen Okaikue-Woodi et al. 2020).

Many cities are endeavoring to prevent sewer overflows and slow urban stormwater by implementing decentralized stormwater controls such as low-impact developments and green stormwater infrastructure (Read et al. 2019, Sun et al. 2014). These "best management practices" (BMPs) include management systems like permeable pavement (porous surfaces that allow

stormwater to infiltrate into the soil or in groundwater), bioretention basins (shallow landscaped depressions that collect stormwater runoff and filter the water through soil and vegetation), and vegetated swales (channels used to transport runoff that help slow runoff, facilitate infiltration, and filter pollutants) (EPA 2021, WSDOT 2014). Due to the multiple benefits of installing these systems (i.e., increased local groundwater recharge and mitigated street flooding), King County and Seattle Public Utilities incentivize property owners in Seattle to install cisterns and rain gardens on private property through a rebate program known as "RainWise" (King County 2021). BMPs can help reduce demand on public stormwater drainage systems and conserve water resources by reducing runoff volumes (Loperfido et al. 2014). Additionally, BMPs can remove particulate bound contaminants (Yu, Yu, and Xu 2013). However, BMPs have proven unable to sufficiently treat many of the dissolved contaminants in stormwater when conventional materials such as sand, gravel, and compost are employed (Okaikue-Woodi et al. 2020). For example, Okaikue-Woodi et al. evaluated contaminant removal efficiency for four types of BMPs, showing these BMPs significantly removed suspended solids but struggled with dissolved contaminants. Additionally, many pollutants that are not well tracked and are most likely not well removed by current BMPs either (Spahr et al. 2020. This is especially true considering the growing number of complex, synthetic chemicals released into the environment which are even resistant to removal and degradation in engineered aquatic systems (Masoner 2019).

1.3 Engineered Media

To treat trace contaminants in urban stormwater, engineered media is being investigated to replace or mix with conventional media in BMPs (L. Zhang et al. 2010, Charbonnet et al. 2018, Randall and Bradford 2013). Engineered media refers to materials like sand, clays, or organic materials that have been physically or chemically altered to enhance contaminant removal). Typical removal methods include separating contaminants (i.e., removal via adsorption) and degradation of contaminants (i.e., oxidation) (Rajapaksha 2016). Most engineered media under investigation seek to physically remove or adsorb contaminants in urban stormwater. To be effective, engineered media must have the ability to remove a broad suite of contaminants and have high reactivity and long lifetimes under realistic urban stormwater conditions. Additionally, engineered media must not impede the flow of stormwater as one of the main focuses of BMPs is to remove runoff from roads quickly. Examples of emerging engineered media are coated sands, modified zeolites, and polymer clay composites (Okaikue-Woodi et al. 2020).

1.4 Biochar

One engineered media that has shown to be particularly promising is biochar: a carbonaceous porous material produced by pyrolyzing a biomass feedstock in a low oxygen atmosphere (Lehmann 2009). Biochar has proven capable of removing a variety of contaminants through adsorption including nutrients, heavy metals, bacteria, and trace organic contaminants (Ashoori et al. 2019, Mohanty and Boehm 2014). Biochar has a high surface area and porosity which facilitates contaminant adsorption onto surface sites and diffusion into pore spaces (Chen et al. 2017). Additionally, biochar surface properties such as surface charge and surface functional groups (carboxyl, hydroxyl, phenolic hydroxyl, and carbonyl groups) provide a variety of avenues for contaminant removal (Nartey and Zhao 2014). For example, biochar removes nutrients by acting as an electron carrier. Trace metal removal occurs via electrostatic (ion) attraction and surface

complexation with oxygen containing functional groups, and microbial and trace organic contaminant removal is achieved through diffusion and hydrophobic interactions as biochar high carbon content imparts a large degree of hydrophobicity (Nartey and Zhao 2014, Reddy, XIE, and Dastgheibi 2014). Biochar can be chemically activated to increase microporosity, surface area, and the density of oxygen-containing functional groups (Linares-Solanol et al. 2012). Potassium hydroxide (KOH) is commonly used activation agent for carbonaceous materials (such as activated carbon) due to high reactivity and stability allowing it to react with relatively inert materials such as carbon (Linares-Solanol et al. 2012). Additionally, the pyrolysis temperature for biochar can vary the surface area and higher temperatures and reduce the amount of oxygen-containing functional groups on the biochar's surface (Rajapaksha 2016). Biochar's surface area dramatically increases when heated above 400°C but remains constant or starts decreasing after 900°C (Chen et al. 2017).

Biochar used for stormwater applications can be produced from a variety of feedstock materials such as wood or corn (Zhao 2019). For biochar to be successful in stormwater BMP applications, it is important for the feedstock material to be low cost and widely available. This thesis explores the viability of spent coffee grounds as a biochar feed material. Spent coffee grounds are an excellent choice for a feed material due to their high carbon content, mechanical strength, availability worldwide, and ease of acquisition as spent coffee grounds are often separated from other food waste products (Kim 2014). For example, Starbucks® provides free spent coffee grounds diverted from their other waste to consumers with their "Grounds for your Garden" program. Locally, coffee grounds are abundant as coffee is the one of the most popular beverages in the Pacific Northwest: Starbucks locations in Seattle alone have been estimated to generate 12 tons of spent coffee grounds daily. Two spent coffee ground (SCG) biochars were investigated in this study: (i) a biochar pyrolyzed at 400°C (so-called "SCG 400") to generate a charcoal-like product; and, (ii) a chemically altered biochar prepared by activating the SCG 400 biochar in the presence of potassium hydroxide (so-called "SCG KOH") biochar. The use of spent coffee grounds as a biochar feedstock for urban stormwater media amendments can offer an economical, sustainably produced, highly effective solution to addressing urban stormwater pollution.

2. Objectives and Hypotheses

This thesis has three main objectives: The first objective of the study aims to convert and characterize spent coffee grounds to a biochar adsorbent media. It is hypothesized that the highly carbonaceous and mechanical strength properties of spent coffee grounds will enable ideal biochar characteristics. The second objective for this study is to determine biochar removal capacity (both activated with KOH and non-activated) for individual contaminants, mixed contaminant systems, and natural organic matter through batch sorption studies. The batch sorption studies also aim to examine the effects of the simulated stormwater mixture (SSM) on biochar contaminant removal. It is likely that the NOM will compete for bonding sites on the biochar reducing the contaminant adsorption. Conversely, divalent cations in the SSM will likely increase adsorption via electron bridging. Higher adsorption rates are expected from the more hydrophobic compounds. Finally, the third objective aims to quantify the removal potential and lifetime of KOH modified biochar produced from spent coffee grounds through column studies. The modified biochar is expected to exhibit high removal rates over long lifetimes.

3. Methods and Materials

3.1 Preparation of SCG biochar

3.1.1 Accumulation and Drying

To begin producing biochar, spent coffee ground feedstock material for the biochar was obtained from the University of Washington Bay Laurel Catering Services from their industrial drip coffee makers which use Starbucks® Pike Place® grounds, a medium roast, arabica coffee sourced from Latin America. The grounds were obtained directly after use and immediately dried at 90°C for 42 hours to remove excess moisture and stored in an airtight container to prevent molding. The grounds were sieved to obtain a grain size range from 595 µm (NO. 30) to 841 µm (NO. 20) to ensure higher retention of grain sizes above 297 µm (NO. 50) throughout the pyrolysis stages.

3.1.2 SCG 400 Biochar Production

The carbonization of the SCG to create the SCG 400 biochar (non-activated biochar) was achieved using the Thermcraft Compact Split Tube Furnace, eXPRESS LINE Protégé (Model XST-2-0-12-1V1-E28) while completing the following procedures. Two quartz boats were filled with approximately 4g of SCG until the boats were full but not overflowing to prevent spillage while in the tube furnace. The boats were loaded into the process tube with a furnace handle hook until the boats were centered in the furnace while ensuring the individual samples were not touching and were not extended beyond the inside edge of the furnace insulation. Alumina insulation blocks were placed in both ends of the process tube such that the outside edge of the block was approximately 2 inches from the edge of the tube. The ends of the process tube were sealed with steel flanges and rubber O-rings to create an airtight environment within the process tube. Influent tubing was attached to the left side of the process tube and a flow meter. More influent tubing was then attached from the flow meter to a nitrogen gas cylinder. Effluent tubing was attached to the right side of the process tube and placed in deionizer water to scrub combustion products from the effluent gas. **Figure 3.1** shows the finished furnace set-up. The nitrogen gas turned on to a flow rate of 500 mL/min and the process tube was purged for 10-15 minutes to ensure a fully nitrogenous atmosphere. The furnace was plugged in and turned on using the switch located on the bottom right corner of the back of the furnace. The furnace was then programmed to first heat the material to 200°C at a ramp rate of 10°C/min and held at that temperature for one hour to facilitate complete evaporation of water from the SCG pore spaces and then heated to 400°C at the same ramp rate for 4 hours to carbonize the coffee grounds. Finally, once the furnace and material were fully cooled, the SCG 400 was sieved again to obtain only the grain sizes between 297 µm (NO. 50) and 841 µm (NO. 20).

Figure 3.1 Thermcraft Tube Furnace with a sealed quarts process tube, nitrogen tank, flow meter, and influent and effluent tubing.

3.1.1 SCG KOH Activated Biochar Production

Chemical activation of the SCG 400 was performed using potassium hydroxide (KOH). The SCG 400 and KOH were added to quartz boats in a 1:1 ratio with the potassium hydroxide spread evenly throughout the SCG 400. The quartz boats were then loaded into the furnace with the same methods as listed in the *Section 3.1.2*. The furnace was then programmed to first heat the material to 200°C at a ramp rate of 10°C/min and held at that temperature for one hour to facilitate complete evaporation of water from the SCG 400 pore spaces and then heated to 800°C at the same ramp rate for 30 minutes to melt and distribute the KOH. Once the furnace and material were fully cooled, the SCG KOH was washed repeatedly with 0.002% HCl until a pH of 7 was reached. The SCG KOH was dried at 90°C for 24 hours to remove excess moisture and sieved to obtain only the grain sizes above 297 µm.

3.1.4 Biochar Characterization

Proximate carbon analyses of the SCG feedstock, SCG 400, and SCG KOH were completed using the method detailed in ASTM D1762-84 (reapproved 2007) (2007; Mukherjee et al., 2011). The specific surface area of the SCG 400 and SCG KOH biochars were evaluated from nitrogen adsorption data collected at 77 K using a Micromeritics 3Flex instrument and the Brunauer-Emmett-Teller (BET) surface area method. Surface zeta potential measurements were completed to determine the surface charge of SCG 400 and SCG KOH using a Zetasizer Nano ZS (Malvern Instruments, UK).

3.2 Stormwater Mixture

The stormwater mixture used in the column and batch sorption were prepared with a simulated stormwater mixture, natural organic matter, and the trace contaminants of interest. The simulated stormwater mixture included the following constituents and constituent concentrations as described by Ray et al (**Table 3.1**).

Table 3.1 Simulated stormwater matrix representing realistic anion and cation concentrations in stormwater (Ray et al. 2019)

Constituent	Concentration (mM)
Ca^{2+}	0.75
Mg^{2+}	0.075
Na^{+}	1.75
NH_4^{+}	0.072
SO_4^{2-}	0.33
HCO_3^{-}	1.00
Cl^{-}	1.70
NO_3^{-}	0.072
$H_2PO_4^{-}$	0.016

The stock solutions of the simulated stormwater mixture were prepared by separating the anions and cations to prevent precipitation. Magnesium chloride hexahydrate ($MgCl_2.6H_2O$), calcium chloride dihydrate ($CaCl_2.2H_2O$) and ammonium chloride (NH_4Cl) were used as representative cations in the simulated stormwater matrix. Sodium sulfate (Na_2SO_4), sodium bicarbonate ($NaHCO_3$), sodium nitrate ($NaNO_3$) and sodium phosphate monobasic monohydrate ($NaH_2PO_4.H_2O$) served as representative anions in the simulated stormwater mixture.

Humic acid from Sigma Aldrich was used to represent natural organic matter (NOM) in the stormwater at a concentration of 10 mg-C/L. Humic acid was chosen instead of the Suwannee River NOM (SRNOM) standard as large volume of NOM was needed to complete all tests and SRNOM was financially restrictive. Humic acid provides an acceptable NOM proxy as the dominant organic matter expected in biochar applications is terrestrially derived organic carbon. Humic acid concentrations were measured using a Sievers Total Organic Carbon (TOC) analyzer.

The trace contaminants used were atrazine (ATR), caffeine (CAF), diuron (DIU), fipronil (FIP), and pentachlorophenol (PCP) and the concentrations varied depending on the test. The contaminants were chosen to represent a wide range of hydrophobicity (**Table 3.2**) among organic compounds commonly found in urban stormwater to determine if the SCG KOH has selective adsorption affinities for more hydrophobic compounds.

Table 3.2 Properties of trace organic contaminants used in batch sorption and column analyses including typical stormwater concentrations (TSC) (Masoner et al. 2019) and reference dose (RfD) (EPA 2020).

Compound	Structure	MW (g/mol)	Purity	TSC (ng/L)	RfD (mg/kg/day)	Log K_{ow}
Caffeine, CAF (wastewater pollution indicator)	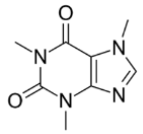	194.19	N/A	1,000	0.0025	-0.07
Atrazine, ATR (herbicide)	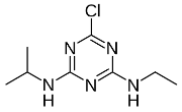	215.68	>97.0%	30	0.002	2.61
Diuron, DIU (herbicide)	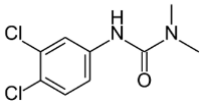	233.09	>98.0%	50	0.003	2.68
Fipronil, FIP (insecticide	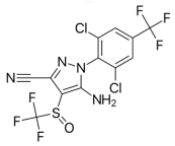	437.15	97.5%	15	0.0002	4.00
Pentachlorophenol, PCP (herbicide)	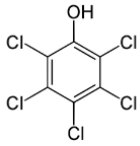	266.33	97.0%	400	0.005	5.12

The organic contaminant concentrations were measured using liquid chromatography-mass spectrometry (LC-MS) analytical chemistry technique while using diuron-d6 and pentachlorophenol-13C6 internal standards to account for sample loss and instrument variability. LC-MS analysis methods are detailed in **Appendix A.1**

3.3 Batch Sorption Tests

The adsorption capacities of SCG 400 and SCG KOH were evaluated through single and multipollutant studies as well as through isotherm batch sorption tests. Additionally, the trace organic compound adsorption rates on SCG 400 and SCG KOH were evaluated through batch kinetic tests. Each batch sorption test was run in triplicates and with control samples (i.e., no adsorbent) and dosed with 1 g/L of biochar. After each batch sorption test was completed, samples were filtered with a 0.22 um filter and mixed with diuron-d6 and pentachlorphenol-13C6 internal standards in LC-MS vials for LC-MS analysis. This approach was used for all batch sorption tests to quantify trace organic contaminant concentrations. No syringe filtration was performed for the column studies.

3.3.1 Adsorption Capacity

The adsorption capacity batch sorption tests (**Table 3.3**) were used to evaluate the impact of trace contaminant adsorption onto the biochar from each individual element of the column studies. The adsorption capacity tests were dosed with contaminants at 50 µg/L. All adsorption capacity tests were mixed with 1g/L of biochar for 5 days. For certain single and mixed pollutant studies, a Milli-Q water was used in place of the simulated stormwater matrix. The adsorption of NOM by SCG 400 and SCG KOH in test #4 was evaluated using a Sievers Total Organic Carbon (TOC) analyzer.

Table 3.3 Adsorption capacity batch sorption test parameters including presence of natural organic matter (NOM) and a simulated stormwater matrix (SSM).

Batch Sorption Test	Biochar Type	Contaminant System	Contaminant Concentration	NOM	SSM
1	SCG 400	Individual	50 µg/L	N/A	No
1	SCG KOH	Individual		N/A	No
2	SCG 400	Mixed		N/A	No
2	SCG KOH	Mixed		N/A	No
3	SCG 400	Mixed		N/A	Yes
3	SCG KOH	Mixed		N/A	Yes
4	SCG 400	Mixed	N/A	10 mg-C/L	Yes
4	SCG KOH	Mixed	N/A		Yes
5	SCG 400	Mixed	50 µg/L		No
5	SCG KOH	Mixed			No
6	SCG 400	Mixed			Yes
6	SCG KOH	Mixed			Yes

3.3.2 Adsorption Isotherms

The isotherm tests were used to evaluate the maximum adsorption capacity of SCG KOH biochar. In the isotherm tests, the contaminants were dosed as listed in **Table 3.4.** All isotherm tests were

mixed with 1g/L of SCG KOH biochar for 5 days. For isotherm study, the SSM also contained a humic acid concentration of 10 mg-C/L.

Table 3.4 Isotherm batch sorption tests parameters with varying contaminant concentrations in the presence of natural organic matter (NOM) and a simulated stormwater matrix (SSM).

Batch Sorption Test	Biochar Type	Contaminant System	Contaminant Concentration	NOM	SSM
7	SCG KOH	Mixed	25 µg/L	10 mg-C/L	Yes
7			75 µg/L		
7			100 µg/L		
8			250 µg/L		
8			750 µg/L		
8			1,000 µg/L		
9			2,500 µg/L		
9			7,500 µg/L		
9			10,000 µg/L		

3.3.3 Adsorption Kinetics

The batch sorption kinetics tests were used to evaluate the rate of adsorption of the five trace contaminants (CAF, ATZ, DIU, FIP, and PCP). The kinetics tests were dosed with 50 µg/L of each contaminant and mixed with 1g/L of SCG KOH biochar. Sampling was performed after for 1 minute, 5 minutes, 10 minutes, 30 minutes, 1 hour, 12 hours, 24 hours, and 5 days of reaction. The SSM with 10 mg-C/L humic acid was used for all kinetics studies.

3.4 Column Building

Bench scale column tests were conducted to compare the contaminant removal performance of biochar as a function of weight percentage (wt%). Sand only columns were prepared as controls of 0.5 wt% and 3 wt% biochar-amended test columns. Triplicates of all columns were used for statistical analysis of all the column data (**Figure 3.2**). The columns were constructed using SCH 40 (1.125" inner diameter) PVC pipe cut to 6" and pipe fittings from McMaster Carr. The pipe fittings were sealed and connected to the PVC pipe with Oatey Medium Black ABS Cement. Fine mesh was glued inside the pipe fitting to prevent sand from washing out of the columns. Each column was packed by filling the lower pipe fitting with pea gravel, then adding sand or the sand and biochar mixtures (at 0.5 wt% and 3 wt%) until the PVC pipe was full, and then adding the upper pipe fitting filled with pea gravel. The columns were connected to an outlet drainage pipe.

The pump was calibrated to find the pumping speed for 1 mL/min to mimic realistic infiltration rates (Gregory et al. 2006). The columns were then flushed with deionized water for 24 hours at the lowest pump setting and any leaks were sealed with Oatey Medium Black ABS Cement.

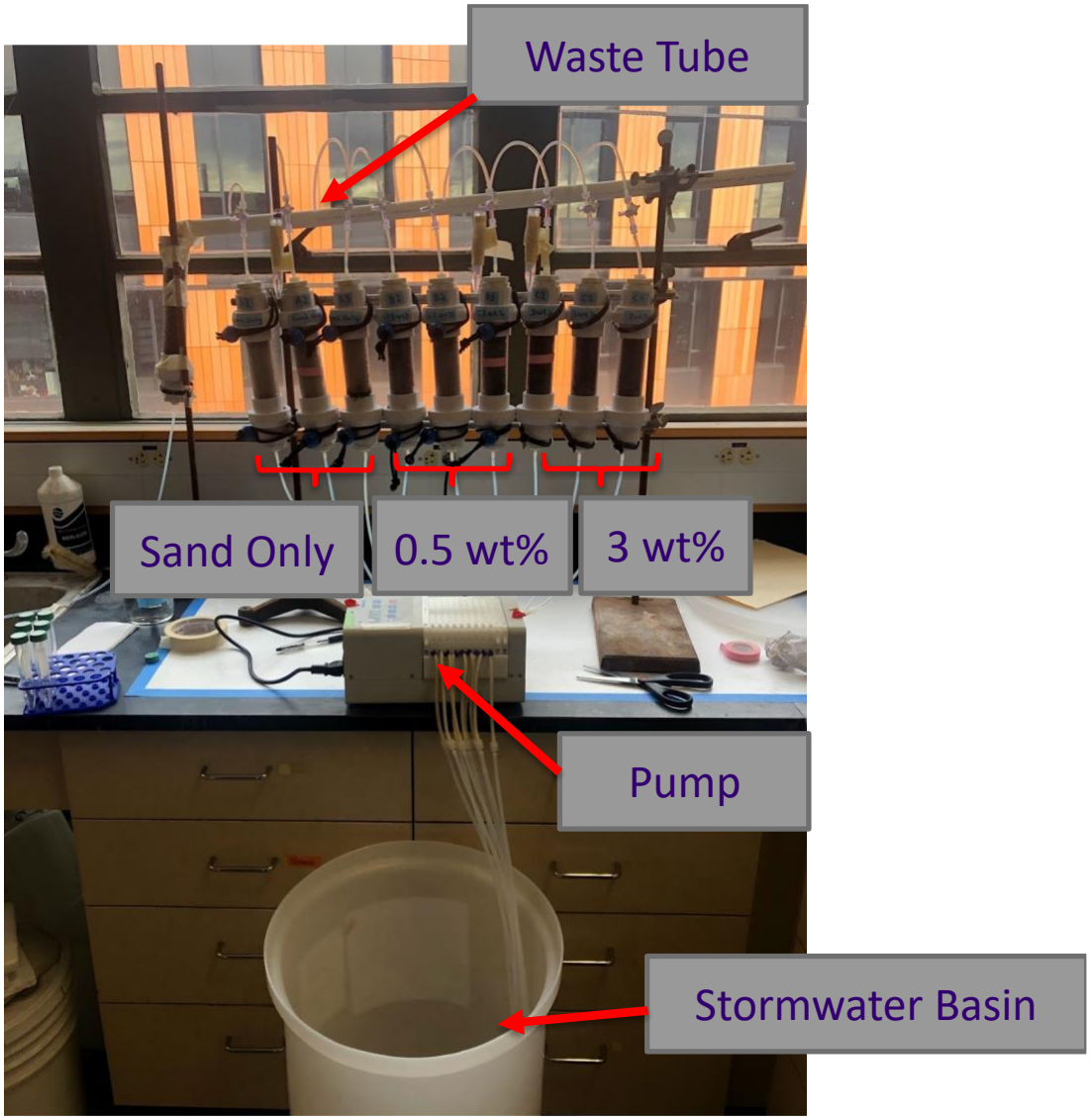

Figure 3.2 Column study set-up with stormwater mixture intake basin, pump, all nine columns, and the outlet drainage pipe (waste tube).

3.5 Tracer Test

Once the columns were built and flushed with deionized water, a tracer test was performed using a 500 mg/L sodium fluoride solution at a pumping rate of 1 mL/min. The fluoride mixture was pumped through the columns for 20 minutes and then sampled every 4 minutes until the tracer breakthrough peak was detected. The sand only and 0.5 wt % columns had pore volumes of 96 minutes, and the 3.0 wt % columns had a pore volume of 108 minutes at the porosities corresponding to each column and the designated flow rate. The aqueous fluoride concentrations

were measured with a Mettler Toledo perfectION™ Combination Fluoride Electrode. Tracer test data and tracer breakthrough peaks can be found in **Appendix A2**.

4. Results and Discussion

This section includes data on biochar characterization, batch sorption tests, and bench scale column studies.

4.1 Biochar Characterization

Proximate carbon analyses of the SCG feedstock, SCG 400, and SCG KOH showed fixed carbon percentages of 17%, 71.1%, and 84.8 % respectively. Upon pyrolysis and then activation with KOH, the fixed carbon content increased by 318% and then by 19% which indicates an increasing degree of aromaticity and hydrophobicity in the biochar. It was hypothesized that the increased hydrophobicity would contribute to a greater extent of trace organic removal in the batch sorption and column tests. Additionally, The BET surface areas of SCG 400 and SCG KOH were measured as 2.66 m^2/g and 852.11 m^2/g respectively. Upon activation with KOH, the specific surface area increased 31,932% The high surface area of the activated biochar also indicates a high degree of porosity within the media, which will result in an abundance of sorption sites and pathways for contaminant diffusion. Finally, the surface zeta potential analysis reported zeta potentials of -37.8 mV and -52.0 mV for SCG 400 and SCG KOH respectively. While both types of biochar were found to have negative surface charges, SCG KOH measured more negative with the zeta potential increasing by 37.6% after activation with KOH potentially due to the creation of more acid-based surface functional groups upon activation. This negative surface charge suggests SCG 400 and SCG KOH will have high adsorption affinities for positively charged ions.

4.2 Batch Sorption Results

Ten batch sorption tests (including kinetics tests) were completed to test different aspects of the SCG biochar's adsorption capabilities by varying contaminant, contaminant concentration, presence of natural organic matter or simulated stormwater matrix, and mixing time. Batch test results comparing adsorption of organics were plotted as normalized organic contaminant removal (i.e., final concentration (µg/L) divided by initial concentration (µg/L) as a function of the trace organic compound or time.

4.2.1 Adsorption Capacity

The effects of individual ("Individual Cont") and mixed contaminant (i.e., "Mixed Cont") matrices, natural organic matter, and a simulated stormwater matrix ("SSM") on trace organic compound adsorption by the SCG 400 and SCG KOH biochar were first evaluated through batch sorption tests. The trace organics plotted in **Figures 4.1 – 4.3** are in order of increasing log K_{ow} values.

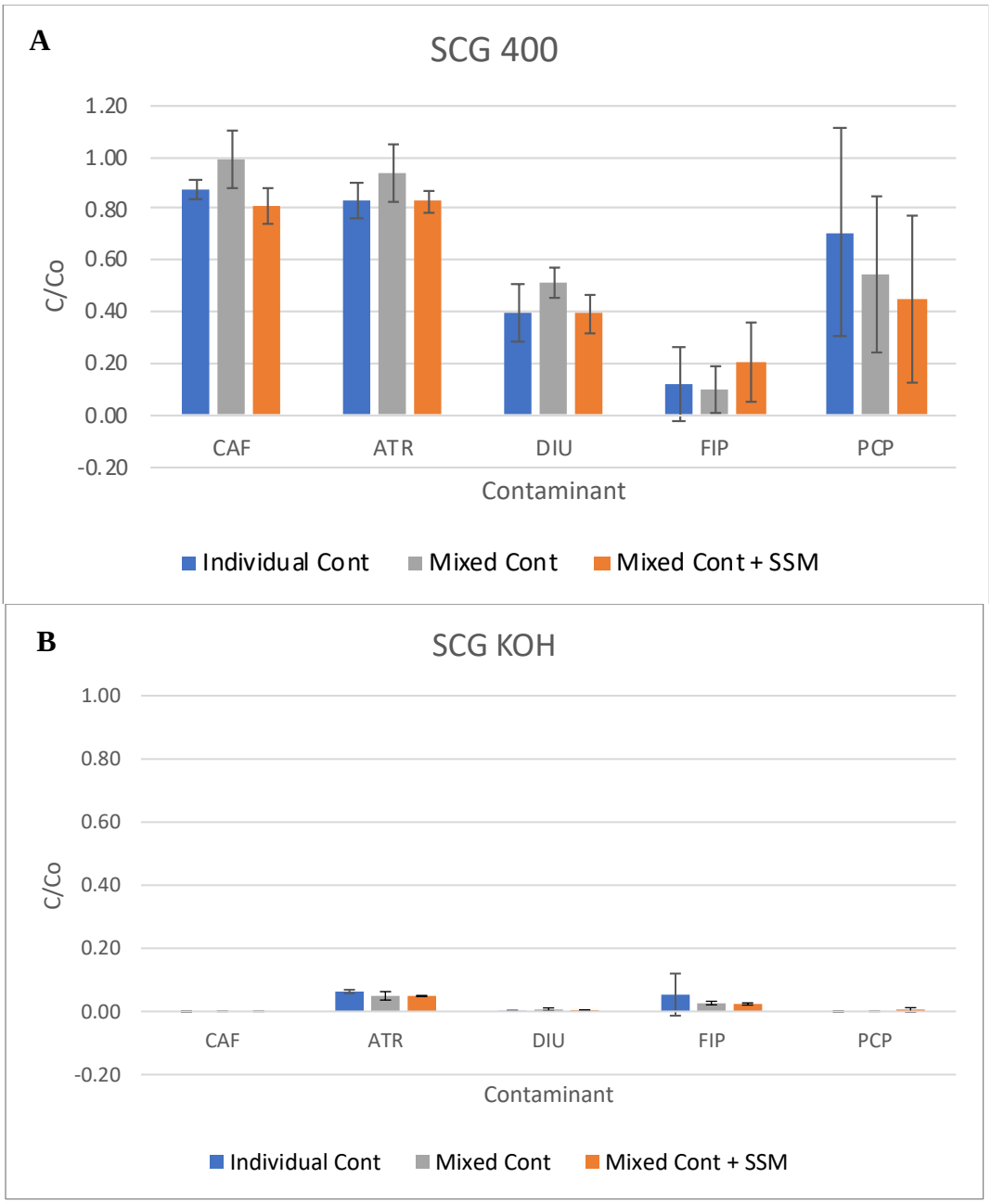

Figure 4.1 5-day batch adsorption results of **A.** 1 g/L SCG 400 or **B.** 1 g/L SCG KOH and 50 µg/L of individual contaminant matrices, 50 µg/L (each) mixed contaminant matrix, and a 50 µg/L (each) mixed contaminant matrix in SSM.

SCG 400 adsorbed low amounts of CAF, ATR, and PCP (15-25%) and higher amounts of DIU and FIP (60-90%). SCG KOH removed nearly all contaminants in the individual contaminant matrix. When compared to the individual contaminant matrix, the SCG 400 biochar removed fewer contaminants when exposed to a mixed contaminant matrix except for the more hydrophobic compounds (FIP and PCP). This trend was expected as the presence of multiple compounds compete for binding sites on the biochar surface. The high variances in FIP and PCP removal are likely due to errors in the data acquisition. When the SSM was added to a mixed contaminant

matrix, SCG 400 removed more contaminants than the batch sorption tests with only a mixed contaminant matrix (apart from FIP) likely due to ion bridging effects from cations in the SSM (Reddy 2014). Overall data tends for SCG 400 showed increased trace organic removal with increased compound hydrophobicity (i.e., log K_{ow}) as hypothesized. PCP was the only contaminant to vary from the trend, but also exhibited the highest standard deviation. This hydrophobic trend likely persisted due to the low porosity and surface area of SCG 400. While there was low or varied contaminant removal efficiencies by the SCG 400 biochar, the SCG KOH biochar exhibited almost complete removal of all trace organics with no preferential adsorption for more hydrophobic compounds. SCG KOH likely exhibited higher removal capabilities compared to SCG 400 due to an increased surface area, higher microporosity, and stronger surface charge.

Next, the adsorption of humic acid ("NOM") by SCG 400 and SCG KOH (**Figure 4.2**) as well as the effects of NOM on SCG 400 and SCG KOH adsorption of a mixed contaminant matrix in the presence and absence of SSM (**Figure 4.3**) were evaluated through batch tests.

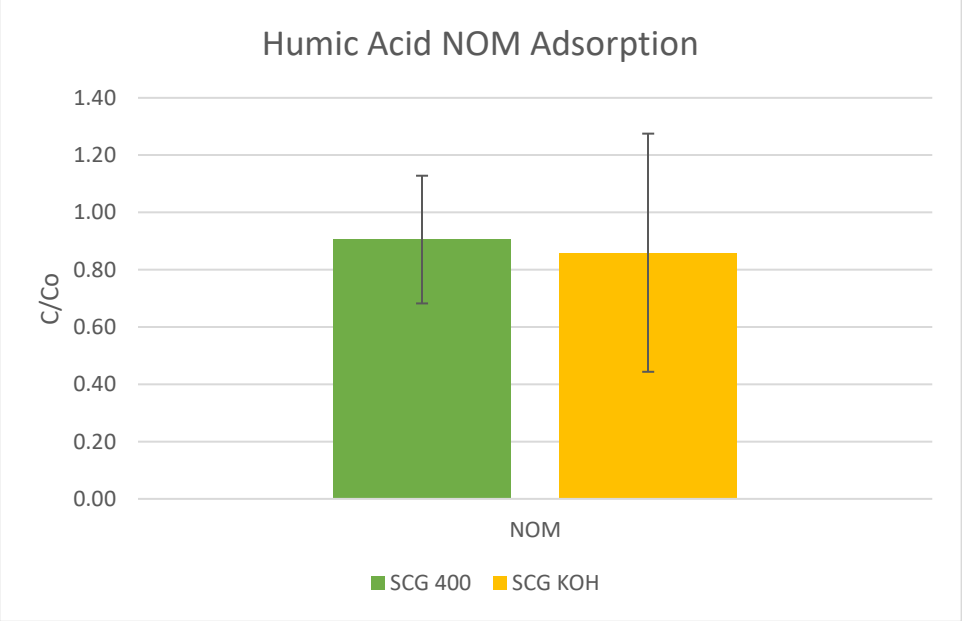

Figure 4.2 5-day batch adsorption results of 10 mg-C/L humic acid NOM by 1 g/L SCG 400 and 1 g/L SCG KOH.

SCG KOH exhibited higher adsorption of natural organic matter which may be attributed to the higher porosity and surface area of the activated biochar. However, high statistical error of the data for SCG KOH adsorption of NOM may indicate further analysis is needed.

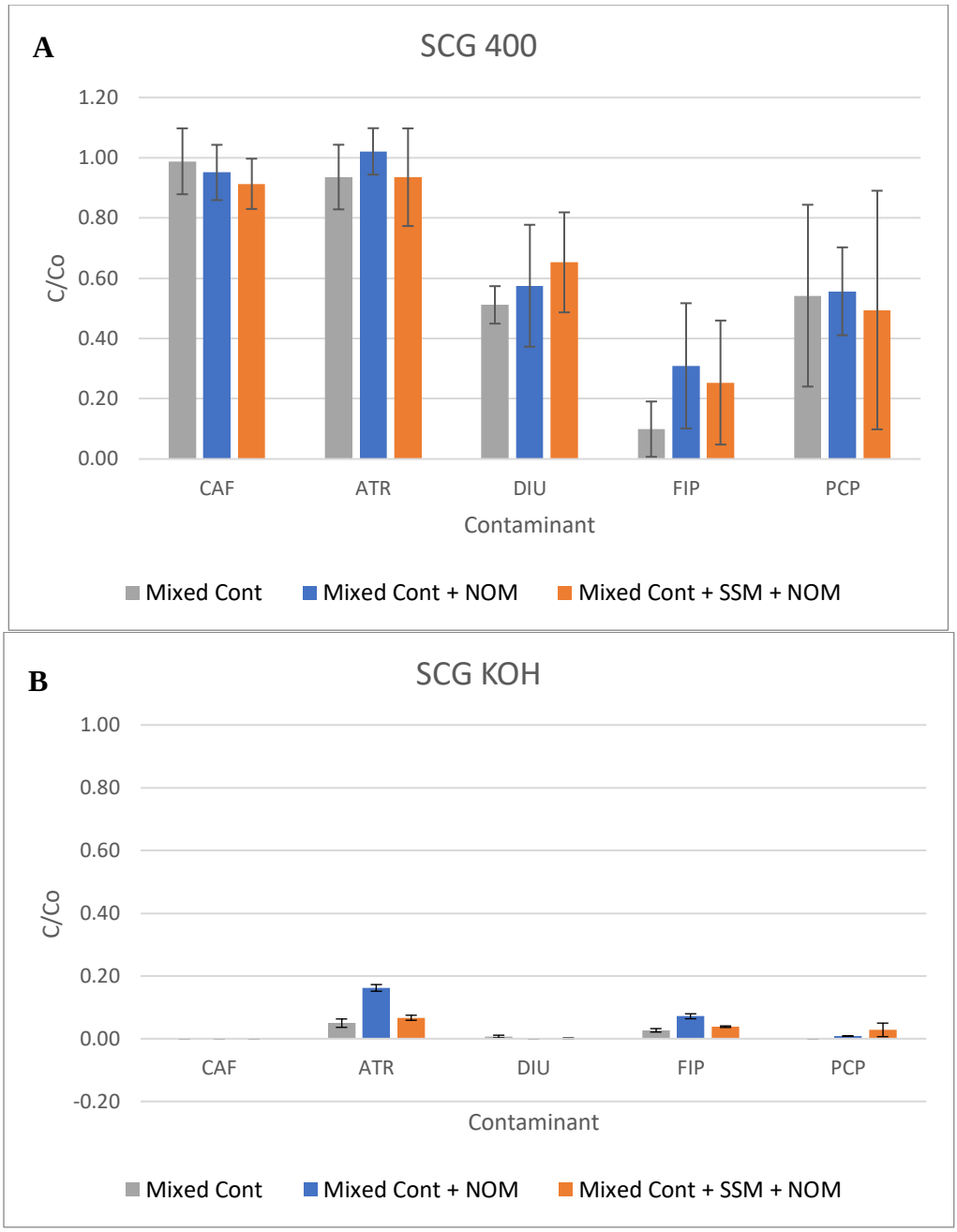

Figure 4.3 5-day batch adsorption results of **A.** 1 g/L SCG 400 or **B.** 1 g/L SCG KOH and 50 µg/L (each) in a mixed contaminant matrix, in the presence of 10 mg-C/L NOM, and in the presence of 10 mg-C/L NOM and the SSM.

The SCG 400 biochar removed fewer contaminants in the mixed contaminant matrix containing NOM (exception: CAF. This trend was expected as hydrophobic compounds compete with hydrophobic NOM for binding sites on the biochar surface. As with the previous batch sorption tests, the high variances in FIP and PCP removal are likely due to errors in the data acquisition. Additionally, when the representative anions and cations in the SSM was added to the mixed contaminant matrix containing NOM, SCG 400 removed more contaminants in the absence of SSM (exception: DIU) likely due to cations in the SSM bridging the negative surface charge of

the biochar and negative organic contaminants. Overall data tends for SCG 400 in these batch sorption tests showed increased removal with increased hydrophobicity as hypothesized. PCP was the only contaminant to vary from the trend, but also exhibited the highest error. This finding was similar to the previous observation in Figure 4.1A comparing trace organic removal in individual and mixed contaminant systems in Milli-Q water. This hydrophobic trend likely persisted due to the low porosity and surface area of SCG 400. SCG KOH exhibited almost complete removal of all trace organics regardless of SSM or NOM addition with no preferential adsorption for more hydrophobic compounds. SCG KOH removed more contaminants than SCG 400 likely due to increases surface area and porosity in the media upon chemical activation.

4.2.2 Isotherm Study

Isotherm batch adsorption test results were plotted as mass of contaminant adsorbed per mass of adsorbent (q_e, mg/g) as a function of final aqueous phase equilibrium contaminant concentration (c_e, µg/L). Approximately 15 mg of activated biochar was mixed for 5 days with contaminant concentrations ranging from 25 µg/L to 10,000 µg/L in 15 mL of SSM and in the presence of NOM. Contaminant ranges were chosen at several orders of magnitude higher than found in actual stormwater conditions to force the adsorption to reach equilibrium to determine the maximum adsorption capacity. The results were fit to Langmuir isotherms (see **Appendix A.3**). The Langmuir fit for caffeine is reported in **Figure 4.4**, while the fits for the remaining contaminants are reported in the appendix **(Appendix Figure A.2).**

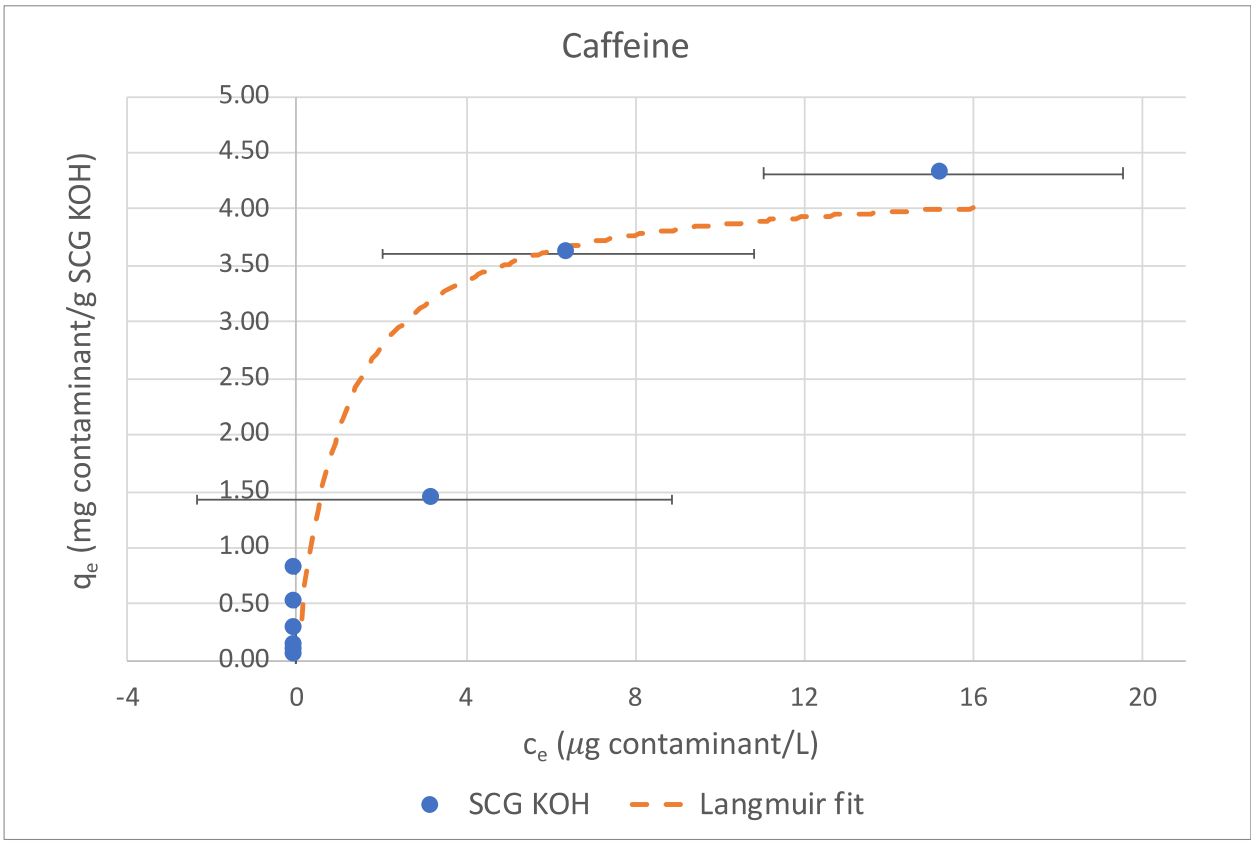

Figure 4.4 Batch adsorption capacity and Langmuir isotherm fit of 1 g/L SCG KOH and varying initial concentrations of caffeine in a SSM with 10 mg-C/L.

Langmuir isotherm fittings resulted in poor correlation with the caffeine equilibrium adsorption data because the SCG KOH removed nearly all contaminants even at the highest examined initial concentrations. A similar finding was observed for the rest of the trace organics. The poor fit for Langmuir and Freundlich isotherms (not reported) suggest that the maximum adsorption capacity for the SCG KOH has yet to be achieved given the range of initial contaminant concentrations (i.e., highest concentration: 10mg/L). However, as the highest contaminant dose used in the isotherm batch sorption tests far exceeded the typical stormwater concentrations for each contaminant ((study: 10,000 µg/L versus real stormwater levels: 1000 ng/L for caffeine), it can be inferred that SCG KOH will have a high removal capacity for trace organic contaminants.

4.2.3 Kinetics

The mass of adsorbed trace organic per mass of SCG KOH was plotted as a function of time *t* to understand the rate of contaminant removal. Kinetic fittings were performed using both the linear pseudo first order ("Linear PFO") and linear pseudo second order ("Linear PSO") models. The fittings and sorption kinetics results for atrazine and caffeine are reported in **Figure 4.5**.

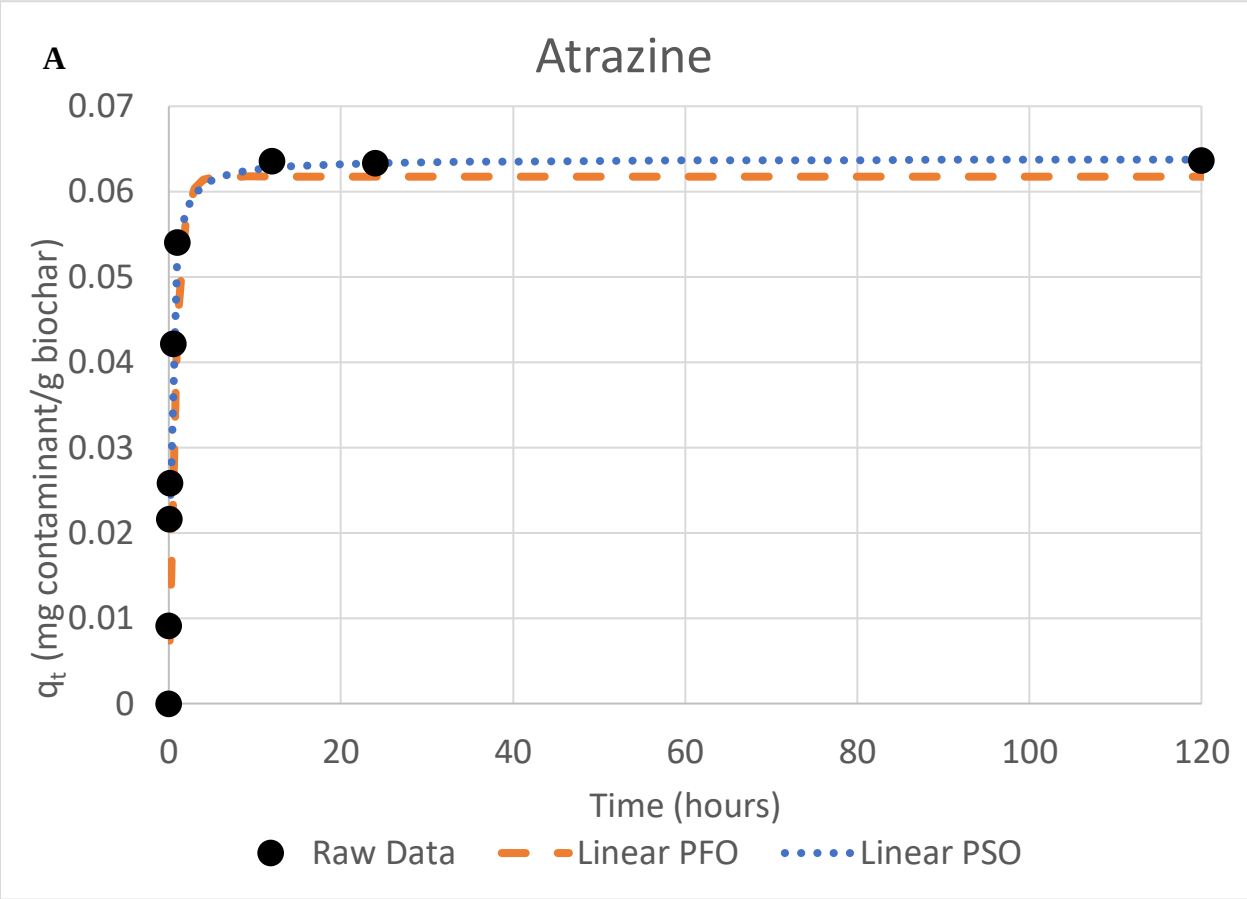

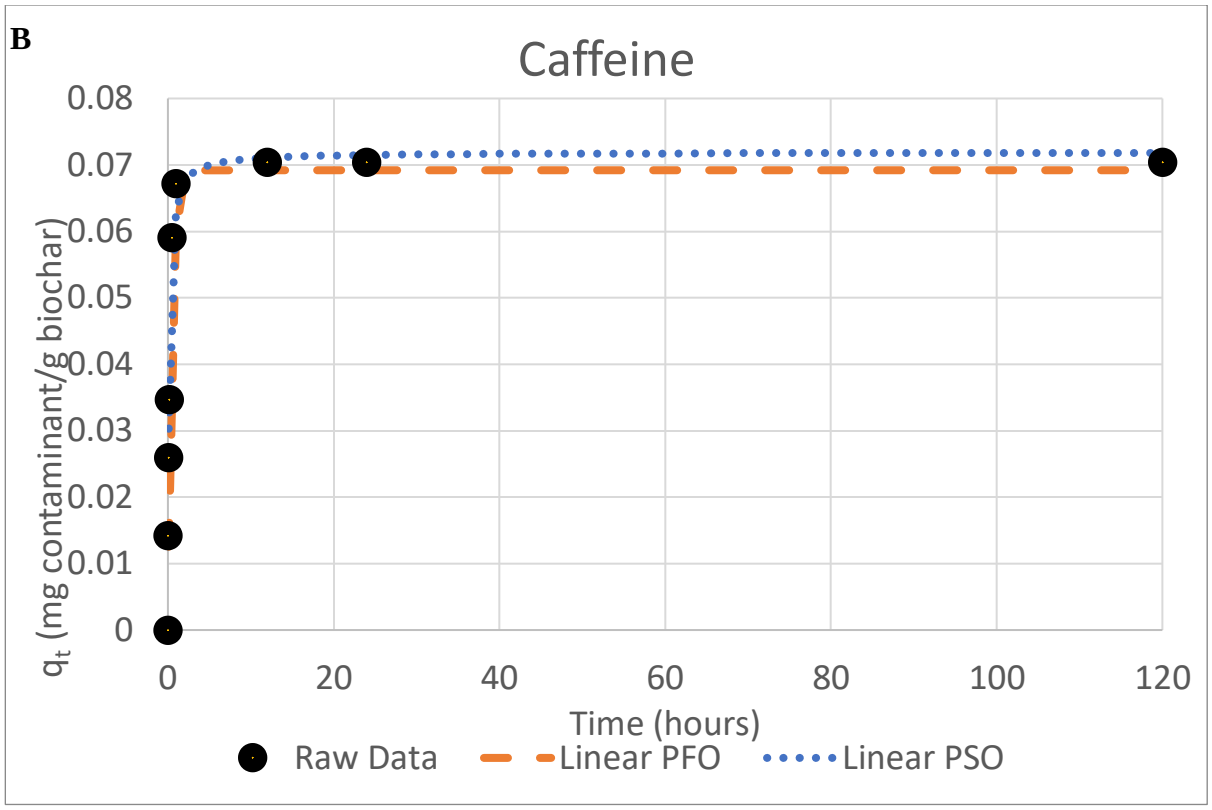

Figure 4.5 Batch kinetics sorption results of 1 g/L SCG KOH50 µg/L of **A.** atrazine and **B.** caffeine in the SSM in the presence of XX mg/L NOM. Fits were performed using linear pseudo first order and pseudo second order models.

Raw data from the kinetic batch sorption tests showed equilibrium adsorption times between 1-12 hours. Additionally, the raw data fit best to a linear PSO fit except for PCP (**Appendix Figure A.3**) which implies the adsorption occurred under conditions relevant to PSO. Once fit with a linear PSO curve, most contaminants were adsorbed by SCG KOH around 4 hours. The rate constants, k_1 and k_2, from the linear PFO and linear PSO fittings respectively (**Table 4.1**)

Table 4.1 Rate constants in hours for the linear pseudo first order (k_1) and linear pseudo second order (k_2) fittings.

Compound	k_1 (h)	k_2 (h)
CAF	3.01	12.1
ATZ	0.24	6.09
DIU	4.22	12.4
FIP	2.44	3.68
PCP	1.08	1.11

As the linear PSO fitting matched the raw data best, the k_2 values indicate PCP had the fastest reaction time while DIU reacted the slowest. The rate constants are higher for the less hydrophobic compounds (CAF, ATZ, and DIU) showing faster adsorption of the more hydrophobic compounds by SCG KOH.

The known octanol-water partition coefficients (log K_{ow}) were compared to a calculated soil adsorption coefficient (log K_d) to determine if biochar had any selective adsorption affinity for the more hydrophobic compounds (**Figure 4.6**).

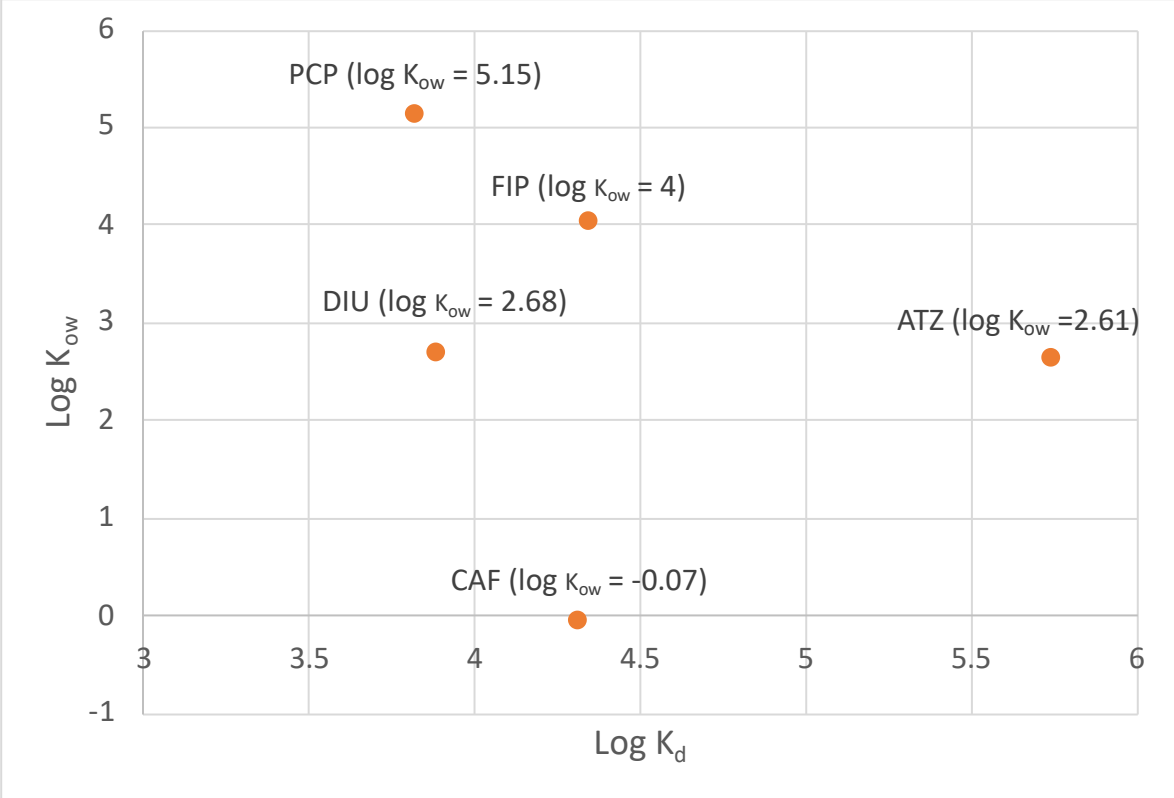

Figure 4.6 Log K_{ow} versus the calculated log K_d for each contaminant.

The log Kd analysis showed no trends of increasing adsorption by biochar for more hydrophobic compounds. This is again consistent with the batch sorption data and shows biochar has high removal capabilities regardless of hydrophobicity.

4.3 Column Studies

Bench scale column testing was conducted with the SCG KOH biochar to investigate adsorption capabilities and lifetime in a more real-world setting. The column studies tested three biochar weight percentages: 0 wt% (sand only), 0.5 wt%, and 3.0 wt%. Each weight percent was tested in triplicates for a total of nine columns. The trace organics plotted in **Figures 4.7 – 4.10** are in order of increasing log K_{ow} values.

4.3.1 Sand Only Columns

The sand only columns (**Figure 4.7**) reached complete breakthrough after 13 pore volumes (1.2 L) of the stormwater mixture.

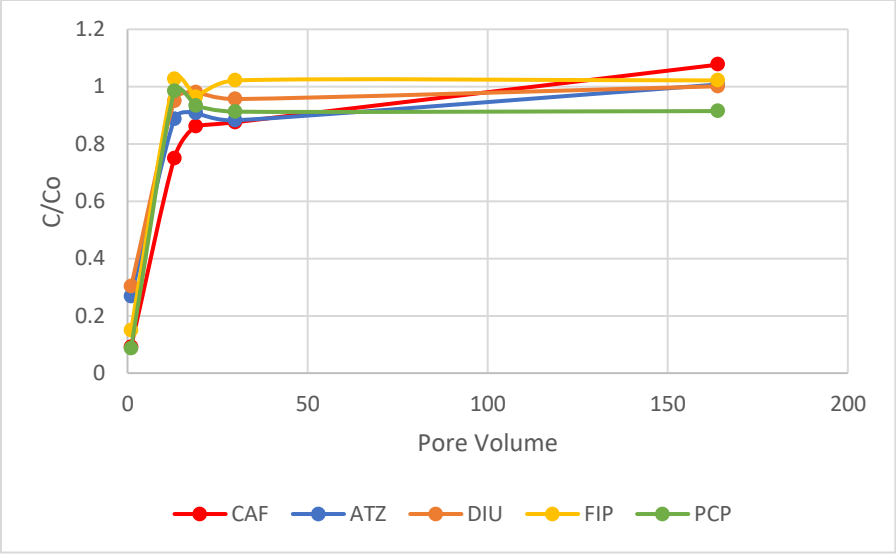

Figure 4.7 Sand only column breakthrough curves plotting normalized contaminant conentration as a function of pore volume. The feed solution contaimed 50 ug/L of each contaminant, 10 mg-C/L NOM, and a SSM.

This quick breakthrough was expected as sand has a low adsorptive capacity for organic contaminants (Barrett 2003).

4.3.2 0.5 wt% Columns

The 0.5 wt% columns (**Figure 4.8**) reached a maximum of 60% breakthrough (according to FIP) after 211 pore volumes (20 L).

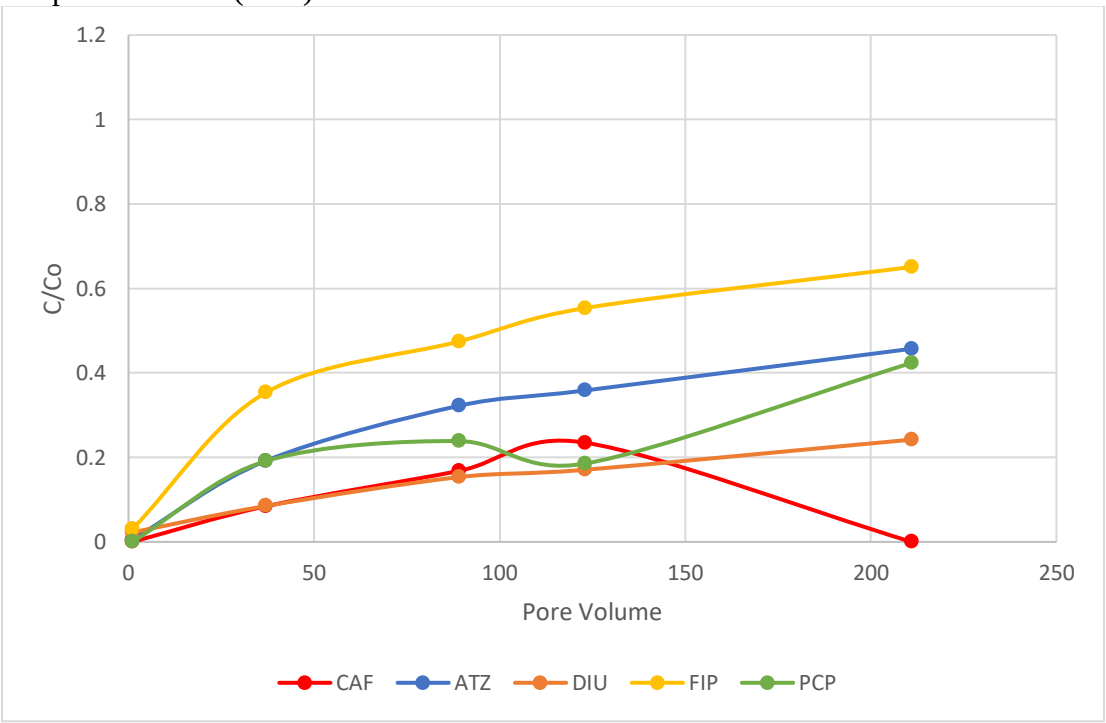

Figure 4.8 0.5 wt% column breakthrough curves plotting normalized contaminant conentration as a function of pore volume. The feed solution contaimed 50 ug/L of each contaminant, 10 mg-C/L NOM, and a SSM.

The variances in data are likely due to inconsistent mixing of biochar in the sand, allowing the development of preferential pathways within the column. These pathways would allow some trace organic contaminants to pass through the length of the column would allow some trace organic contaminants to pass through the length of the column wihout encountering biochar. Lower adsorption affinity for fipronil (more hydrophobic, log K_{ow} =) and higher adsorption affinity for caffeine (less hydrophobic, log K_{ow} = -0.07) contradicted the results from the batch sorption tests. Even at low weight percentages of biochar, there was still high organic contaminant removal over several pore volumes indicating high remocal capacities and potentially long lifetimes of SCG KOH.

4.3.3 3.0 wt% Columns

The 3.0 wt % columns removed 100% of contaminants until 130 pore volumes (16 L) and are continuing to remove nearly 100 % of the less hydrophobic compounds (CAF, ATZ, and DIU) after 1200 pore volumes (**Figure 4.9)** in this ongoing experiment.

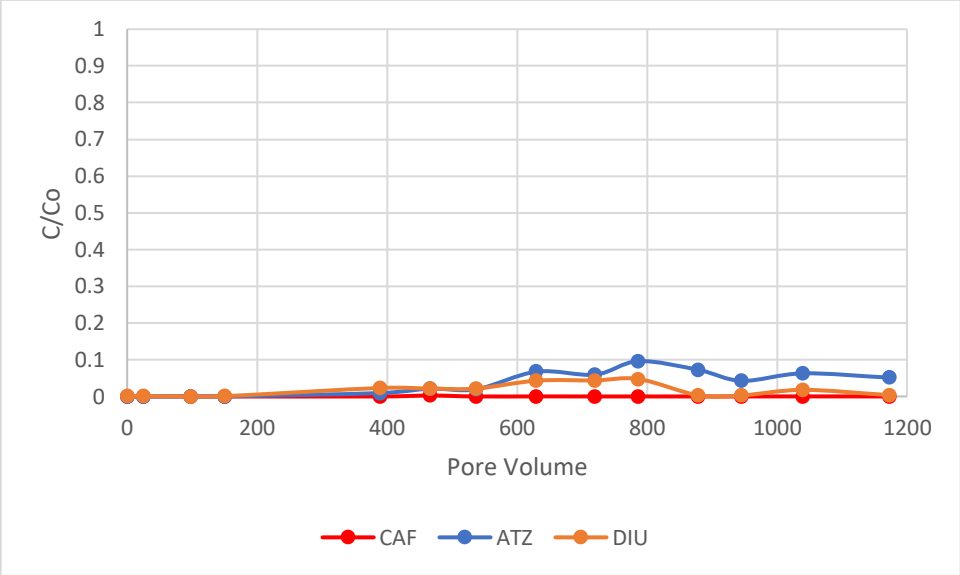

Figure 4.9 3.0 wt% SCG KOH column breakthrough curves plotting normalized contaminant concentration as a function of pore volume for caffeine, atrazine and diuron. The feed solution contained 50 ug/L of each contaminant, 10 mg-C/L NOM, and a SSM.

High adsorption rates of CAF and DIU with slightly lower adsoption of ATZ by SCG KOH were consitent with batch sorption analyses.

The 3.0 wt% columns also continuted to remove nearly 100% of PCP after 800 pore volumes, but did reach 50% breakthrough of FIP after 800 pore volumes (**Figure 4.10**). The adsorption data for FIP and PCP for the 3.0 wt% columns are only reported to 800 pore volumes (versus 1200 for CAF, ATZ, and DIU) as the later LC-MS data for FIP and PCP reported low internal standard areas and could not be used.

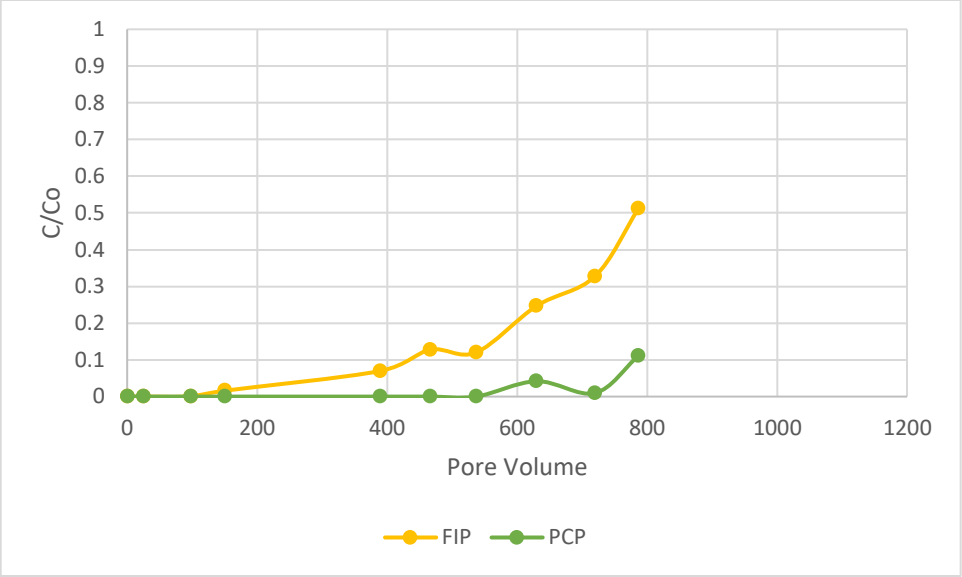

Figure 4.10 3.0 wt% SCG KOH column breakthrough curves plotting normalized contaminant concentration as a function of pore volume for fipronil and pentachlorophenol. The feed solution contained 50 ug/L of each contaminant, 10 mg-C/L NOM, and a SSM.

Lower adsorption affinity for FIP contradicted the results from the adsorption capacity batch sorption tests. Additional analysis of the LCMS data may be needed, and samples will need to be re-analyzed to validate measured concentrations on instrument conditions improve. The results from the column studies show high removal capabilities of the SCG KOH biochar over a wide variety of contaminants for a long lifetime. This is especially true with higher weight percent of biochar amended in the sand columns.

Complete breakthrough for PCP (C/Co = 1) for the 3wt% column was calculated using a polynomial fit on the existing column data. Projections for compete breakthrough of PCP were found to occur after 4262 pore volumes (460L at 50 ug/L for a total of 23,0000 ug). An estimate for a hypothetical rainfall, watershed, and filter design was calculated by Schuler 1987 showing 430 m^3 of runoff for a 5-cm rainfall event over a 1-ha parking area with 90% impermeable surface area. Using the actual stormwater concentration of PCP from Masoner et al. of 400 ng/L gives a total PCP concentration of 430 ug from one storm event. Given this calculation, the 4 grams of biochar used in the 3 wt% columns should be able to treat PCP in a BMP for 53 storm events. This result shows long lifetime potentials of a small amount of biochar. These results would be complicated by the addition of hundreds of contaminants in a typical storm and are calculated from imperfect projections as breakthrough was not reached.

5. Conclusions

The objectives of this work were threefold: (1) converting spent coffee grounds to a biochar adsorbent media and characterizing the product; (2) determining the removal potential of both inactivated and activated spent coffee ground biochar when exposed to individual contaminants, a mixed contaminant matrix, natural organic matter, and a simulated stormwater matrix; and (3) quantifying the removal potential and lifetime of SCG KOH under continuous flow conditions.

These objectives were completed through physical and chemical characterization, batch sorption testing, and bench scale column testing. The key findings of these tests are as follows:

For the first objective: Surface characterizations and element analyses revealed increased surface area through activation and elevated fixed carbon content through pyrolysis. High surface area, porosity, and fixed carbon content and the negative surface charge of SCG KOH were good predictors of removal capabilities for organic contaminants.

For the second objective: Adsorption capacity tests showed competition for binding sites between contaminants on the SCG 400 biochar. The SSM slightly increased SCG 400 adsorption rates for nearly all contaminants. NOM blocked some adsorption sites, leading to lower adsorption on SCG 400 by all contaminants except CAF. Adsorption capacity tests also revealed high adsorption capacities for the activated biochar, as SCG KOH removed nearly all contaminants regardless of contaminant matrix, or NOM/SSM presence. Isotherm batch sorption tests indicated SCG KOH biochar has a high adsorption capacity after removing nearly all contaminants when dosed at 10,000 µg/L. Batch sorption kinetics test showed nearly complete removal of contaminants between 1 and 12 hours, with most contaminants removed by 4 hours. Finally, log Kd versus log Kow analysis resulted in no clear trend between hydrophobicity and SCG KOH biochar adsorption affinity at contaminant concentrations of 50 µg/L.

For the third objective: The columns containing only sand reached complete breakthrough nearly immediately after the tests began. Complete breakthrough occurred after 13 pore volumes, or 1.2 L, indicating low trace organic compound removal capabilities of sand. The columns amended with 0.5 wt% of SCG KOH reached a maximum breakthrough of 60% after 211 pore volumes or 20 L. The columns amended by 3.0 wt % of SCG KOH continued complete removal of all contaminants until 150 pore volumes (16 L). Nearly complete removal of CAF, ATZ, and DIU is still ongoing after 1200 pore volumes (130 L) treated. Meanwhile, breakthrough of FIP reached a maximum of 60% after nearly 800 pore volumes (85 L), and complete removal of PCP is still ongoing after nearly 800 pore volumes (85 L).

Results from all tests show SCG KOH has high removal capabilities of a wide range of organic contaminants for a long lifetime.

6. Recommendations for Future Work

Additional investigations could improve understanding of SCG KOH adsorption capacity and lifetime. Continued sampling of 3 wt% biochar columns until final breakthrough is reached as well as breakthrough projection calculations could provide better insight into SCG KOH biochar lifetimes. Mesocosm-scale experiments would be appropriate to further investigate biochar in real world conditions and potentially with effects from intermittent flow. Expanding tests to include trace metals, nutrients, and other types of contaminants would help gain better insight into the extend of SCG KOH biochar adsorption capacities. Increasing the yield of SCG KOH through larger furnaces would increase the viability of use in pilot scale applications. Finally, disposal methods for spent material should be investigated to ensure safe disposal of biochar after trace contaminant adsorption.

7. References

Ashoori, N., Teixido, M., Spahr, S., LeFevre, G. H., Sedlak, D. L., Luthy, R. G. (2019). Evaluation of pilot-scale biochar-amended woodchip bioreactors to remove nitrate, metals, and trace organic contaminants from urban stormwater runoff. *Water Research, 154*, 1-11

Barrett Michael E. 2003. Performance, Cost, and Maintenance Requirements of Austin Sand Filters. *Journal of Water Resources Planning and Management 129* (3): 234–42.

Berndtsson, Justyna C. (2010). Green Roof Performance towards Management of Runoff Water Quantity and Quality: A Review. *Ecological Engineering, 36*(4), 351–360.

Center for Watershed Protection (CWP). (2003). "Impacts of impervious cover on aquatic systems" *Watershed Protection Research Monograph No. 1., Center for Watershed Protection.* https://clear.uconn.edu/projects/TMDL/library/papers/Schueler_2003.pdf

Chow, M. I., Lundin, J. I., Mitchell, C. J., Davis, J. W., Young, G., Scholz, N. L., McIntyre, J. L. (2019). An urban stormwater runoff mortality syndrome in juvenile Coho salmon. Aquatic Toxicology. 214. https://doi.org/10.1016/j.aquatox.2019.105231

Charbonnet, Joseph A., Yanghua Duan, Case M. van Genuchten, and David L. Sedlak. 2018. "Chemical Regeneration of Manganese Oxide-Coated Sand for Oxidation of Organic Stormwater Contaminants." *Environmental Science & Technology 52* (18): 10728–36.

Chen, Y., Zhang, X., Chen, W., Yang, H., Chen, H. (2017). The structure evolution of biochar from biomass pyrolysis and its correlation with gas pollutant adsorption performance. *Bioresource Technology 246* 101-109. https://doi.org/10.1016/j.biortech.2017.08.138.

ECOSS. (2019). "Combined sewer overflow: how stormwater became Puget Sound's #1 source of pollution." https://ecoss.org/combined-sewer-overflow-stormwater-pollution-gsi-explainer/#:~:text=Seattle%20implemented%20its%20first%20centralized,stormwater%20through%20the%20same%20pipe.&text=Sewage%20is%20directed%20to%20a%20water%20treatment%20plant%20during%20dry%20weather.

EPA. (2018). 2018 Edition of the Drinking Water Standards and Health Advisories Tables. https://www.epa.gov/sites/production/files/2018-03/documents/dwtable2018.pdf

EPA. (2021). "Stormwater Management Practices at EPA Facilities." https://www.epa.gov/greeningepa/stormwater-management-practices-epa-facilities

Feist, B. E., Buhle, E. R., Baldwin. D. H., Spromberg, J. A., Damm, S. E., Davis, J. W., Scholz, N. L. (2017). Roads to ruin: conservation threats to sentinel species across an urban gradient. *Ecological Applications 27*(8), 2382-2396.

Gaffield, S. J., Goo, R. L., Richards, L. A., & Jackson, R. J. (2003). Public health effects of inadequately managed stormwater runoff. *American Journal of Public Health, 93*(9), 1527–1533. https://doi.org/10.2105/ajph.93.9.1527

Gasperi, Johnny, Bastien Laborie, and Vincent Rocher. (2012). Treatment of Combined Sewer Overflows by Ballasted Flocculation: Removal Study of a Large Broad Spectrum of Pollutants. *Chemical Engineering Journal 211-212* (November): 293–301.

Göbel, P., C. Dierkes, and W. G. Coldewey. 2007. "Storm Water Runoff Concentration Matrix for Urban Areas." *Journal of Contaminant Hydrology 91*(1-2): 26–42.

Gregory, J.H., Dukes, M.D., Jones, P.H. and Miller, G.L. (2006) Effect of urban soil compaction on infiltration rate. *Soil Water Conserv*. 61(3), 117-124.
Hogan, Dianna M., and Walbridge Mark R. (2007). Best Management Practices for Nutrient and Sediment Retention in Urban Stormwater Runoff. *Journal of Environmental Quality, 36*(2), 386-395. https://doi.org/10.2134/jeq2006.0142.

Hagekhalil, A. P.E., Kharaghani, S. P.E., Tam, W. P.E., & Haimann, R. P.E. (2014). *City of Los Angeles- The Green Blue City One Water Program*. [Paper presentation]. International Conference on Sustainable Infrastructure: Long Beach California.
https://doi.org/10.1061/9780784478745.045

Kim, M., Hyun-Gi Min, Namin Koo, Jeongsik Park, Sang-Hwan Lee, Gwan-In Bak, Jeong-Gyu Kim, (2014). The effectiveness of spent coffee grounds and its biochar on the amelioration of heavy metals-contaminated water and soil using chemical and biological assessment. Journal of Environmental Management 146, 124-130.https://doi.org/10.1016/j.jenvman.2014.07.001.

King County. (2020). *Executive Constantine unveils 2021-2022 budget, call for major investment in housing, advancing an anti-racist agenda.*
https://kingcounty.gov/elected/executive/constantine/news/release/2020/September/22-budget-release.aspx

King County. (2021). Be RainWise.
https://kingcounty.gov/services/environment/wastewater/cso/rainwise.aspx

Knudson, T., & Vogel, N. (1997). Graphic by Scott Flodin. *The Gathering Storm Part II, Bad land-use policies invite a catastrophe.* The Sacramento Bee.
www.sacbee.com/static/archive/news/projects/gathering_storm/floodplains.html

Lee, Jun H., and Bang, Ki W. (2000). Characterization of Urban Stormwater Runoff. *Water Research 34*(April): 1767-1772

Lehmann, S. J. (2009). *Biochar for Environmental Management*, Earthscan, Oxford, UK.

Linares-Solano, A., Lillo-Ródenas, M. A., Marco-Lozar, M. P., Kunowsky, M., Romero-Anaya, A. J. NaOH and KOH for preparing activated carbons used in energy and environmental applications. *International Journal of Energy, Environment and Economics 20*(4), 59-91

Loperfido, J.V., Noe, G. B., Jarnagin, S. T., Hogan, D. M. (2014). Effects of distributed and centralized stormwater best management practices and land cover on urban stream hydrology at the catchment scale. *Journal of Hydrology. 519*, 2584-2595, https://doi.org/10.1016/j.jhydrol.2014.07.007.

Masoner, J., Kolpin, D., Cozzarelli, I., Barber, L., Burden, D., Foreman, W., Forshay, K., Furlong, E., Groves, J., Hladik, M., Hopton, M., Jaeschke, J., Keefe, S., Krabbenhoft, D., Lowrance, R., Romanok, K., Rus, D., Selbig, W., Williams, B., Bradley, P. (2019). Urban stormwater: an overlooked pathway of extensive mixed contaminants to surface and grounwaters in the United States. Environmental Science and Technology 53, 10070-10081.

McGrane, Scott J. (2016). Impacts of urbanisation on hydrological and water quality dynamics, and urban water management: a review. *Hydrological Sciences Journal*, 61:13, 2295-2311, DOI: 10.1080/02626667.2015.1128084

Miles, C. (2015). *Stormwater facts*. Encyclopedia of Puget Sound. https://www.eopugetsound.org/articles/stormwater-facts#:~:text=The%20total%20amount%20of%20impervious,4.1%25%20of%20the%20total%20basin

Mohanty, S. K., Boehm, A. B., *Escherichia coli* Removal in Biochar-Augmented Biofilter: Effect of Infiltration Rate, Initial Bacterial Concentration, Biochar Particle Size, and Presence of Compost. *Environmental Science and Technology 48*(19), 11535-11542.

Mukherjee, A., Zimmerman, A.R. and Harris, W. (2011). Surface chemistry variations among a series of laboratory-produced biochars. Geoderma 163(3), 247-255.

Nartey, O. D., Zhao, B. (2014). Biochar Preparation, Characterization, and Adsorptive Capacity and Its Effect on Bioavailability of Contaminants: An Overview, *Advances in Materials Science and Engineering*, vol. 2014. https://doi.org/10.1155/2014/715398

Nspiregreen, LLC for DOEE's Stormwater Plan Executive Summary

Okaikue-Woodie, F. E. K, Cherukumilli, K., Ray, J. R. (2020). A critical review of contaminant removal by conventional and emerging media for urban stormwater treatment in the United States. *Water Research* 187. https://doi.org/10.1016/j.watres.2020.116434

Pitt, R., Maestre, A., Clary, J. (2018). The national stormwater quality database version 4.02. Res. Rep. Dep. Civ. Env. Eng. Fac. Eng Saitama Univ.

Rajapaksha, A. U., Season S. Chen, Daniel C.W. Tsang, Ming Zhang, Meththika Vithanage, Sanchita Mandal, Bin Gao, Nanthi S. Bolan, Yong Sik Ok, (2016). Engineered/designer biochar for contaminant removal/immobilization from soil and water: Potential and implication of biochar modification. Chemosphere 148, 276-291. https://doi.org/10.1016/j.chemosphere.2016.01.043.

Randall, Mark T., and Andrea Bradford. 2013. “Bioretention Gardens for Improved Nutrient Removal.” Water Quality Research Journal of Canada 48 (4): 372–86.

Ray, J. R., Shabtai, I. A., Teixidó, M., Mishael, Y. G., Sedlak, D. L. (2019). Polymer-clay composite geomedia for sorptive removal of trace organic compounds and metals in urban stormwater. *Water Research 157*, 454-462.

Read, L. K., Hogue, T. S., Edgley, R., Mika, K. (2019). Impacts of Stormwater Management on Streamflow Regimes in the Los Angeles River. *Journal of Water Resources and Planning*. *145*(10) DOI: 10.1061/(ASCE)WR.1943-5452.0001092

Reddy, K., Xie, T., Dastgheibi, S. (2014). Evaluation of biochar as a potential filter media for the removal of mixed contaminants from urban storm water runoff. Journal of Enviornmental Engineering 140(12).

Sharma, A. K., Vezzaro, L., Birch, H., Arnbjerg-Nielsen, K., and Mikkelsen, P. S. (2016). Effect of climate change on stormwater runoff characteristics and treatment efficiencies of stormwater retention ponds: a case study from Denmark using TSS and Cu as indicator pollutants. *SpringerPlus*, *5*(1), 1984. https://doi.org/10.1186/s40064-016-3103-7

Spahr, Stephanie, Marc Teixidó, David L. Sedlak, and Richard G. Luthy. 2020. “Hydrophilic Trace Organic Contaminants in Urban Stormwater: Occurrence, Toxicological Relevance, and the Need to Enhance Green Stormwater Infrastructure.” *Environmental Science: Water Research & Technology*. *1* https://doi.org/10.1039/C9EW00674E

Sun, Y., Li, Q., Liu, L., Xu, C., Liu, Z. (2014). Hydrological simulation approaches for BMPs and LID practices in highly urbanized area and development of hydrological performance indicator system. *Water Science and Engineering 7*(2), 143-154. https://doi.org/10.3882/j.issn.1674-2370.2014.02.003.

The Nature Conservancy (TNC). “What is Green Stormwater Infrastructure?” Accessed May 15, 2021. https://www.washingtonnature.org/cities/stormwater/green-infrastructure-infographic

United States Geological Survey (USGS). (2021). GLRI Urban Stormwater Monitoring. Accessed May 15, 2021. https://www.usgs.gov/centers/umid-water/science/glri-urban-stormwater-monitoring?qt-science_center_objects=0#qt-science_center_objects

WSDOT. (2014). *Stormwater Best Management Practices.* WSDOT Highway Runoff Manual. Zgheib, Sally, Régis Moilleron, and Ghassan Chebbo. (2012). Priority Pollutants in Urban Stormwater: Part 1-Case of Separate Storm Sewers. *Water Research 46*(20): 6683–92.

Yu, J., Yu, H., and Xu, L. (2013). Performance evaluation of various stormwater best management practices. *Environ Sci Pollut Res 20*, 6160–6171 (2013). https://doi.org/10.1007/s11356-013-1655-4

Zhang, L., E. A. Seagren, A. P. Davis, and J. S. Karns. 2010. “The Capture and Destruction of Escherichia Coli from Simulated Urban Runoff Using Conventional Bioretention Media and Iron Oxide-Coated Sand.” Water Environment Research: A Research Publication of the Water Environment Federation 82 (8): 701–14.

Zhao, J., Shen, XJ., Domene, X. et al. (2019). Comparison of biochars derived from different types of feedstock and their potential for heavy metal removal in multiple-metal solutions. *Sci Rep 9*, 9869 https://doi.org/10.1038/s41598-019-46234-4.

Appendix A

Appendix A.1 LC-MS Analysis

The trace organic compounds used in the batch sorption and column tests were quantified by liquid chromatography- tandem mass spectrometry (LC-MS/MS) using a Waters Quattro Micro quadrupole tandem mass spectrometer and a Phenomenex Gemini NX-C18 column (50 x 3 mm, 3um, 110 A). The mobile phases for the LC consisted of Optima LCMS Grade water with acetonitrile (5%) and acetic acid (1%) (A), and 50% acetonitrile/50% methanol. The gradient is show in Table A1. The mass spectrometer was operated in positive electron mode (for caffeine, diuron, and atrazine) and in negative electron mode (for fipronil and pentachlorophenol) with multiple reaction monitoring modes. Two fragments were selected for each compound one for quantification (Q1) and the other for confirmation (Q2) (**Table A2**). Deuterated diuron and mass-labeled pentachlorophenol were used as internal standards. Samples were filtered using a 0.22 μm syringe filter prior to analysis.

Table A1 Liquid chromatography gradient parameters.

Time (min)	flow rate (mL/min)	% A (94% H2O/ 5% acetonitrile/ 1% acetic acid	% B (50% methanol/ 50% acetonitrile)
0	0.2	90	10
1.5	0.2	45	55
3.5	0.2	36	64
4	0.2	1	99
6	0.2	1	99
6.5	0.3	90	10
9	0.2	90	10

Table A2 Ionization modes and parameters, retention times (RT), and other LC-MS parameters used to quantify concentrations of trace organic contaminants in the batch and column studies.

	Ionization Mode	Parent m/z	Cone Energy (V)	Product Ion (m/z)	Collision Energy (V)	RT (min)
Compounds						
Caffeine	positive	195.15	32	138.25	20	2.93 ± 0.5
				110.15	23	
Atrazine	positive	216.15	35	96.1	25	4.9 ± 0.5
				174.25	17	
Diuron	positive	233	30	45.9	15	5.03 ± 0.5
				71.95	18	
Fipronil	negative	434.9	32	330.2	16	5.56 ± 0.5
		436.9		330.2	16	
Pentachlorophenol	negative	262.85	38	263.1	7	6.86 ± 1.0
		264.85		265.1	7	
Internal standards						
Diuron-d6	positive	239.15	27	52.05	15	5 ± 0.5
				78.05	18	
Pentachlorophenol-13C	negative	272.95	38	273.15	7	6.84 ± 0.5
		270.95		271.15	7	

Appendix A.2 Additional Column Data

Table A3 Weights of each layer of the columns in grams.

	Sand Only Columns	0.5 wt% Columns	3 wt% Columns
Pea Gravel 1 (g)	70	70	60
Sand (g)	145	144.275	140.65
Biochar (g)	0	0.725	4.35
Pea Gravel 2 (g)	65	60	55

Table A4 Tracer test analysis data showing the measured mV with the calculated concentration of fluoride (F-) ions in solution for the sand only, 0.5 wt%, and 3.0 wt% columns. The highlighted data indicates the tracer peak.

	Sand Only		**0.5 wt%**		**3 wt%**	
Time (min)	[F-]	mV	[F-]	mV	[F-]	mV
20	0.1971	87.5	0.0963	105.7	0.0998	104.8
24	0.1084	102.7	0.0711	113.4	0.0598	117.8
28	0.0998	104.8	0.0575	118.8	0.0557	119.6
32	0.0550	119.9	0.0529	120.9	0.0456	124.7
36	0.0754	111.9	0.0467	124.1	0.0431	126.1
40	0.0637	116.2	0.0430	126.2	0.0400	128
44	0.0637	116.2	0.0423	126.6	0.0402	127.9
48	0.0400	128	0.0421	126.7	0.0392	128.5
52	0.1372	96.7	0.0495	122.6	0.0436	125.8
56	0.3368	73.9	0.0600	117.7	0.0443	125.4
60	0.7200	54.6	0.1071	103	0.0511	121.8
64	1.0303	45.5	0.2516	81.3	0.0485	123.1
68	1.4512	36.8	0.6273	58.1	0.0481	123.3
72	1.5455	35.2	1.0887	44.1	0.0810	110.1
76	1.6920	32.9	1.7739	31.7	0.1581	93.1
80	1.9117	29.8	3.1769	16.9	0.3643	71.9
84	2.2555	25.6	5.8487	1.4	0.5844	59.9
88	6.3529	-0.7	9.6434	-11.3	1.2446	40.7
92	8.3689	-7.7	9.6814	-11.4	2.2466	25.7
96	9.7965	-11.7	11.3329	-15.4	5.4058	3.4
100	9.2711	-10.3	11.1119	-14.9	4.9964	5.4
104	8.6367	-8.5	10.5575	-13.6	6.3779	-0.8
108	7.7048	-5.6	9.5678	-11.1	6.9550	-3
112	7.9827	-6.5	8.6028	-8.4	6.6080	-1.7
116	7.3203	-4.3	7.4073	-4.6	6.3529	-0.7
120	7.2059	-3.9	6.6865	-2	6.5304	-1.4
124	6.5047	-1.3	6.3030	-0.5	6.4792	-1.2
128	6.7394	-2.2	5.5569	2.7	5.8718	1.3
132	6.8195	-2.5	6.5562	-1.5	6.0836	0.4
136	5.8487	1.4	5.4058	3.4	5.7800	1.7
140	5.1971	4.4	4.3361	9	5.1361	4.7
144	5.1563	4.6	4.4573	8.3	5.2588	4.1

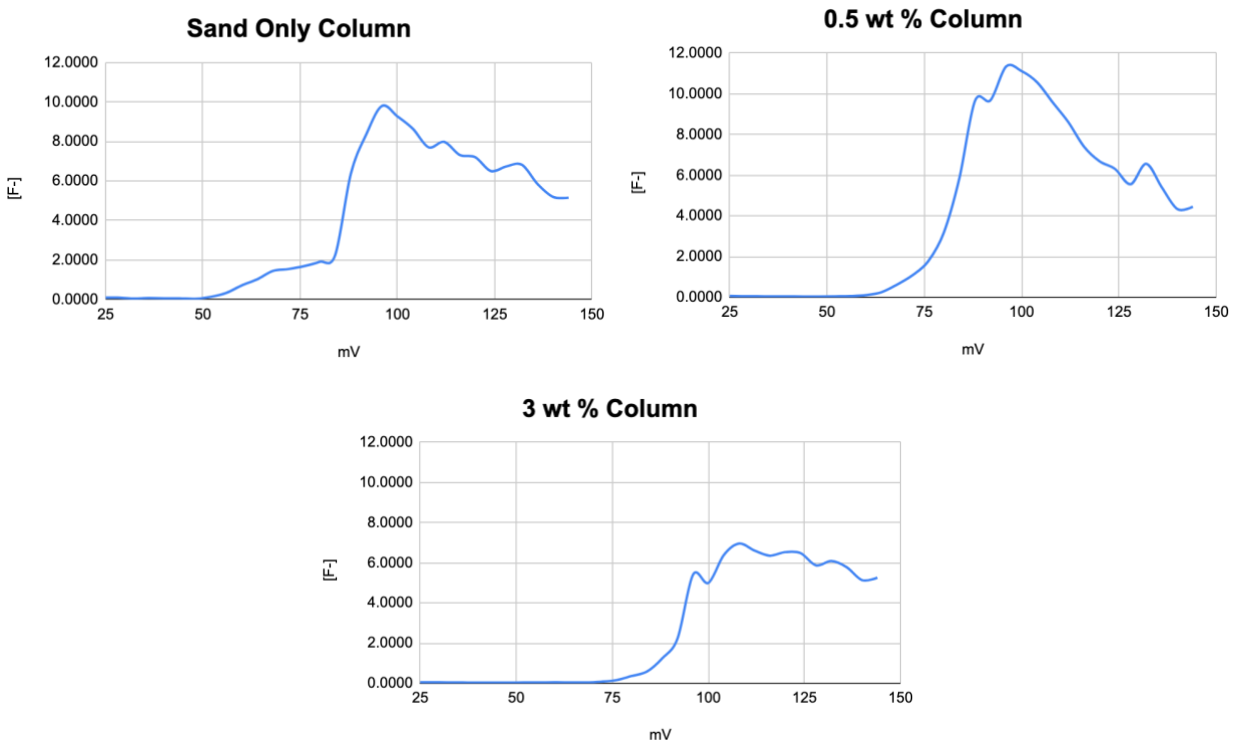

Figure A1 tracer test peaks for the sand only, 0.5 wt%, and 3.0 wt% columns used to determine pore volume time. The feed solution contained 500 mg/L sodium fluoride.

Appendix A.3 Batch Sorption Results

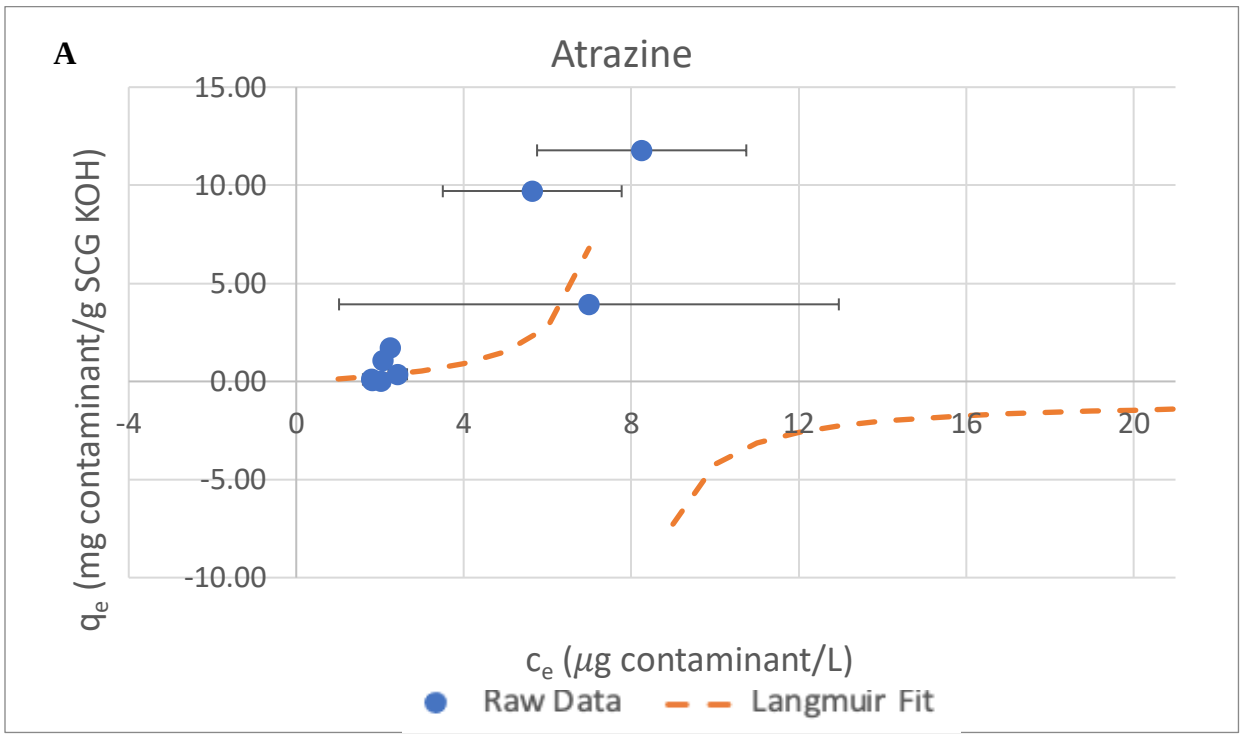

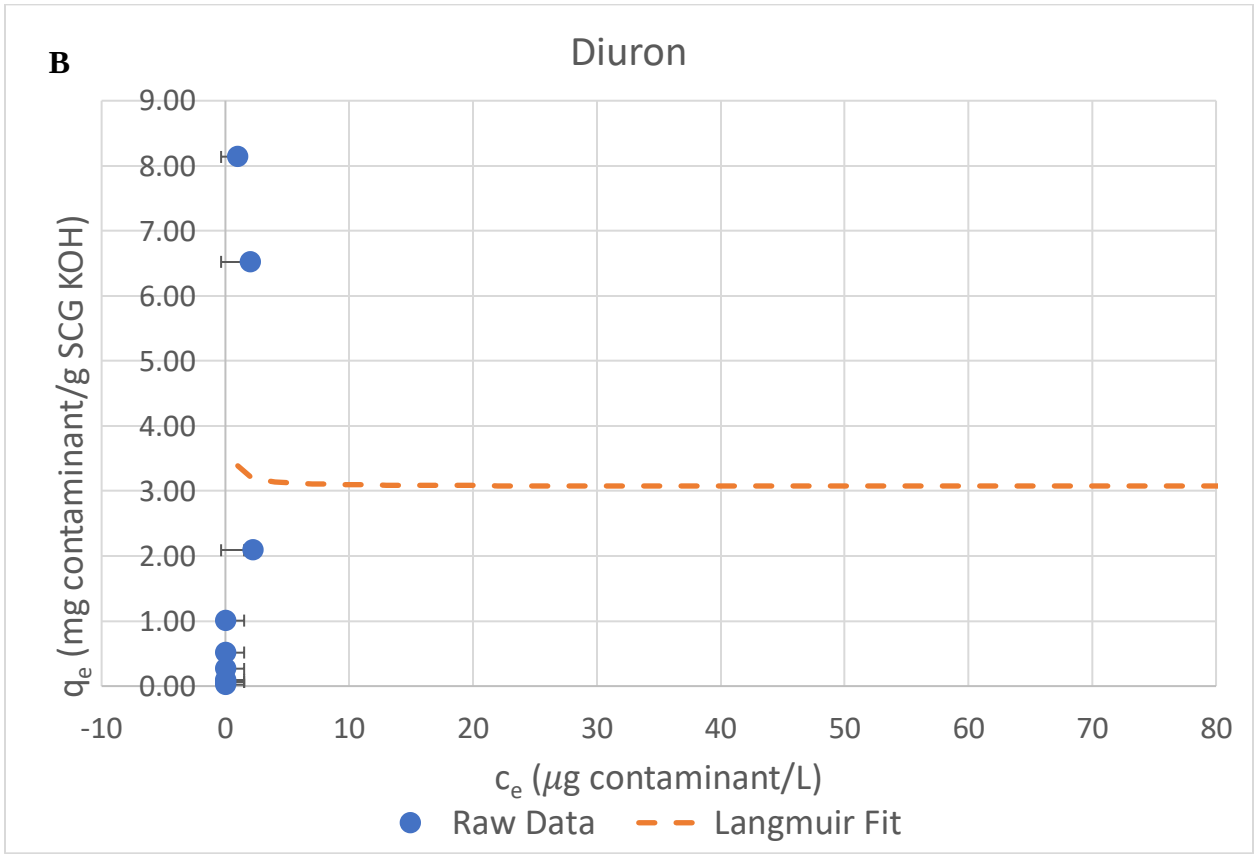

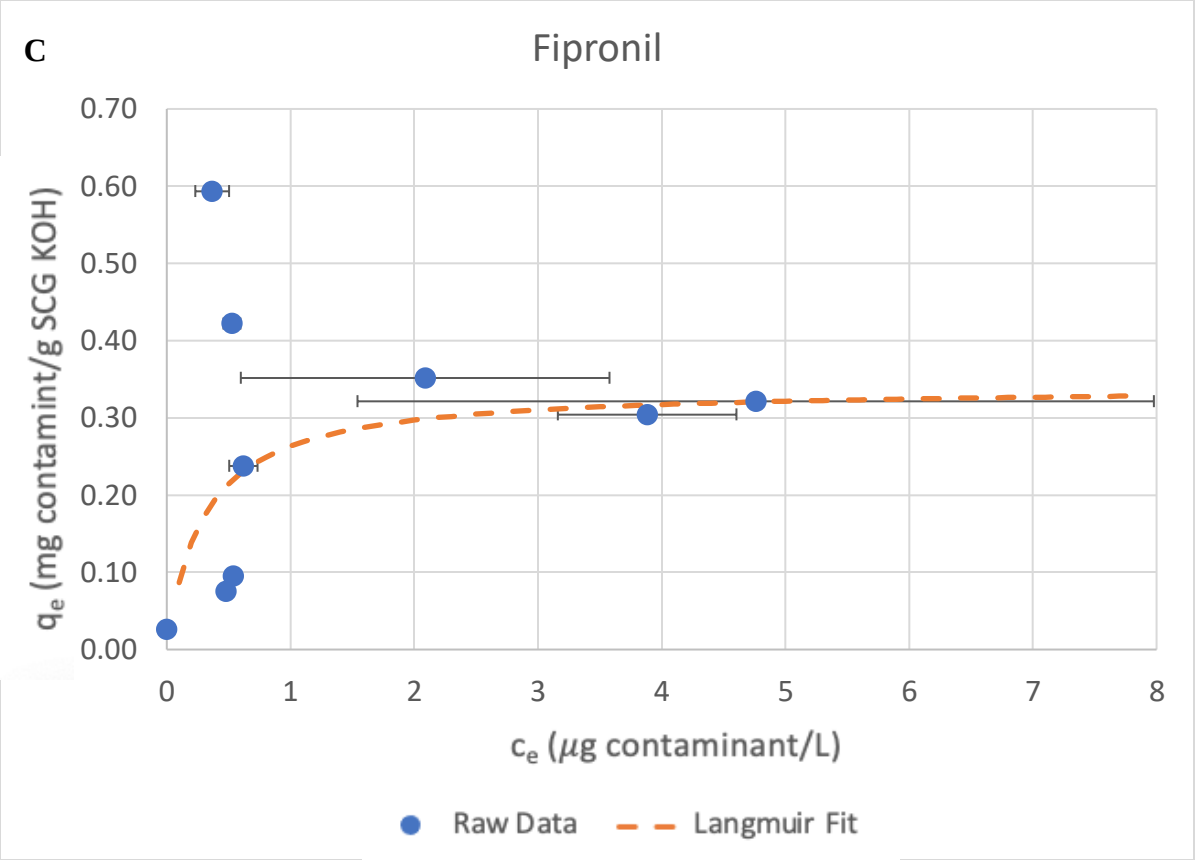

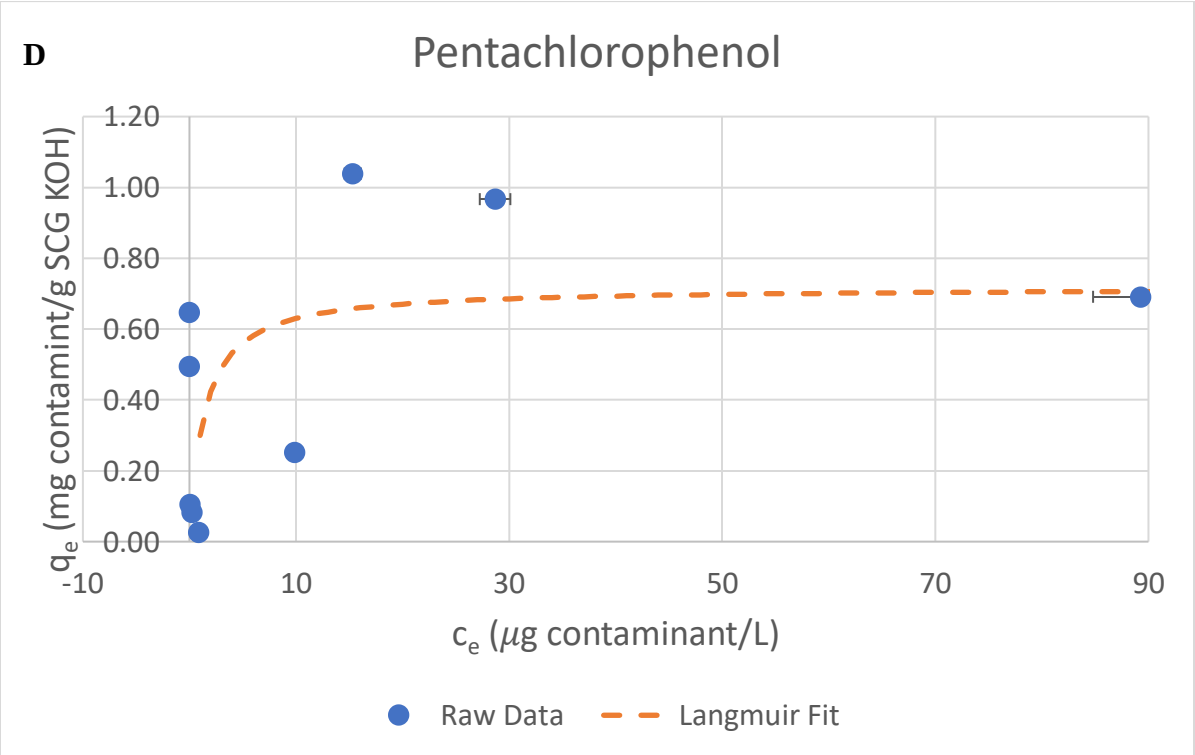

Figure A2 Batch adsorption capacity and Langmuir isotherm fit of 1 g/L SCG KOH and varying initial concentrations of **A**. atrazine, **B.** diuron, **C**. fipronil, and **D**. pentachlorophenol in a SSM with 10 mg-C/L.

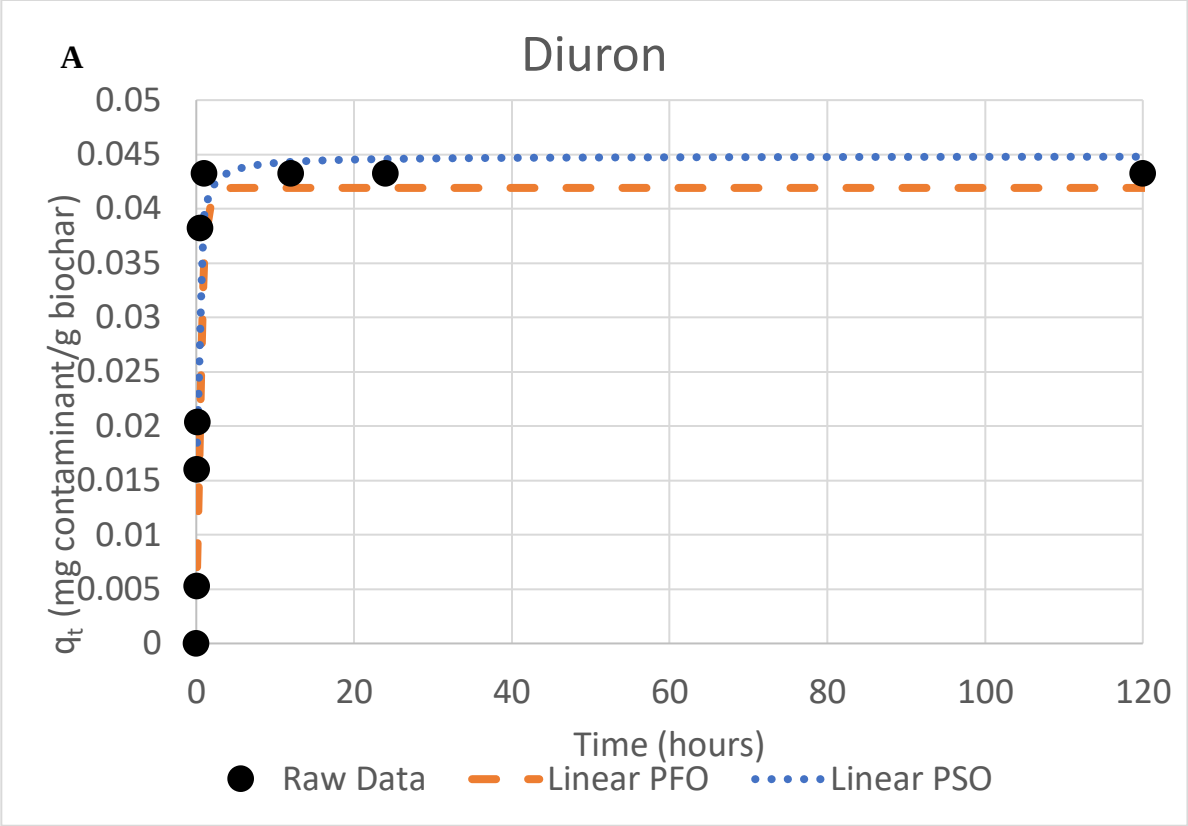
A
Diuron
0.05
0.045
0.04
0.035
0.03
0.025
0.02
0.015
0.01
0.005
0
q_t (mg contaminant/g biochar)
0
20
40
60
80
100
120
Time (hours)
Raw Data
Linear PFO
Linear PSO

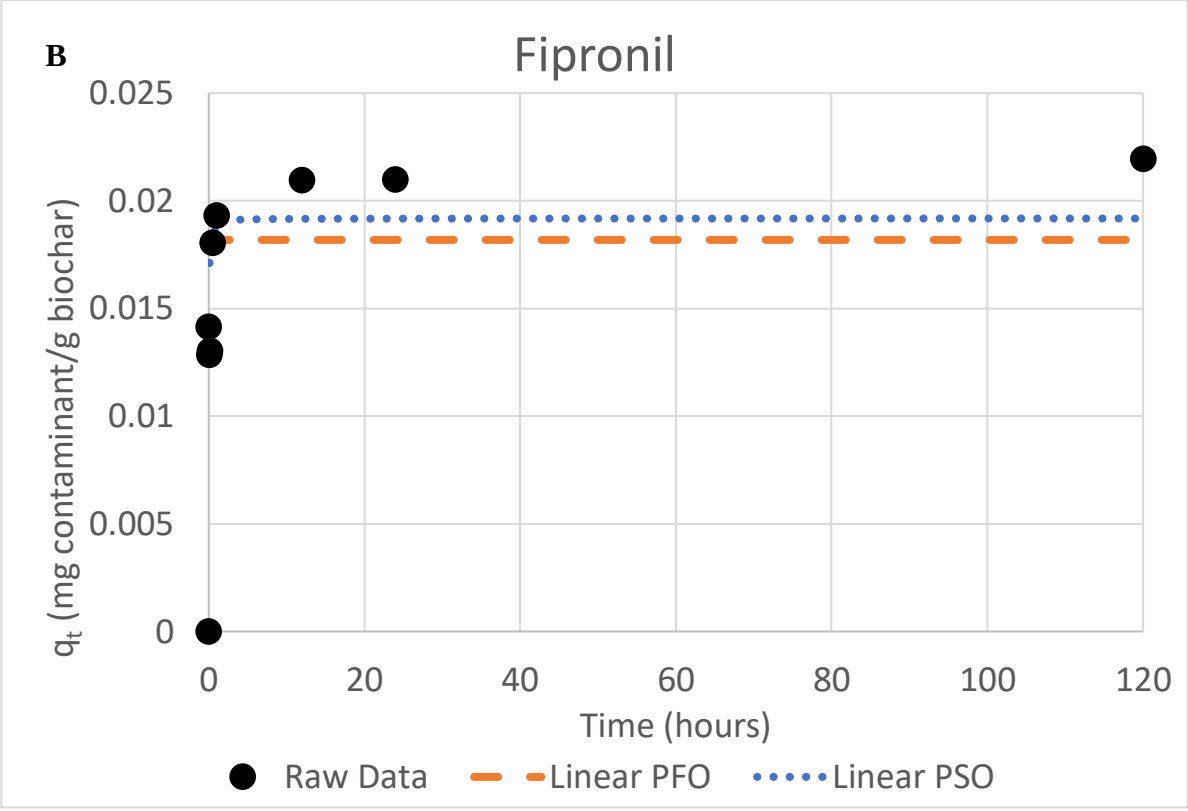
B
Fipronil
0.025
0.02
0.015
0.01
0.005
0
q_t (mg contaminant/g biochar)
0
20
40
60
80
100
120
Time (hours)
Raw Data
Linear PFO
Linear PSO

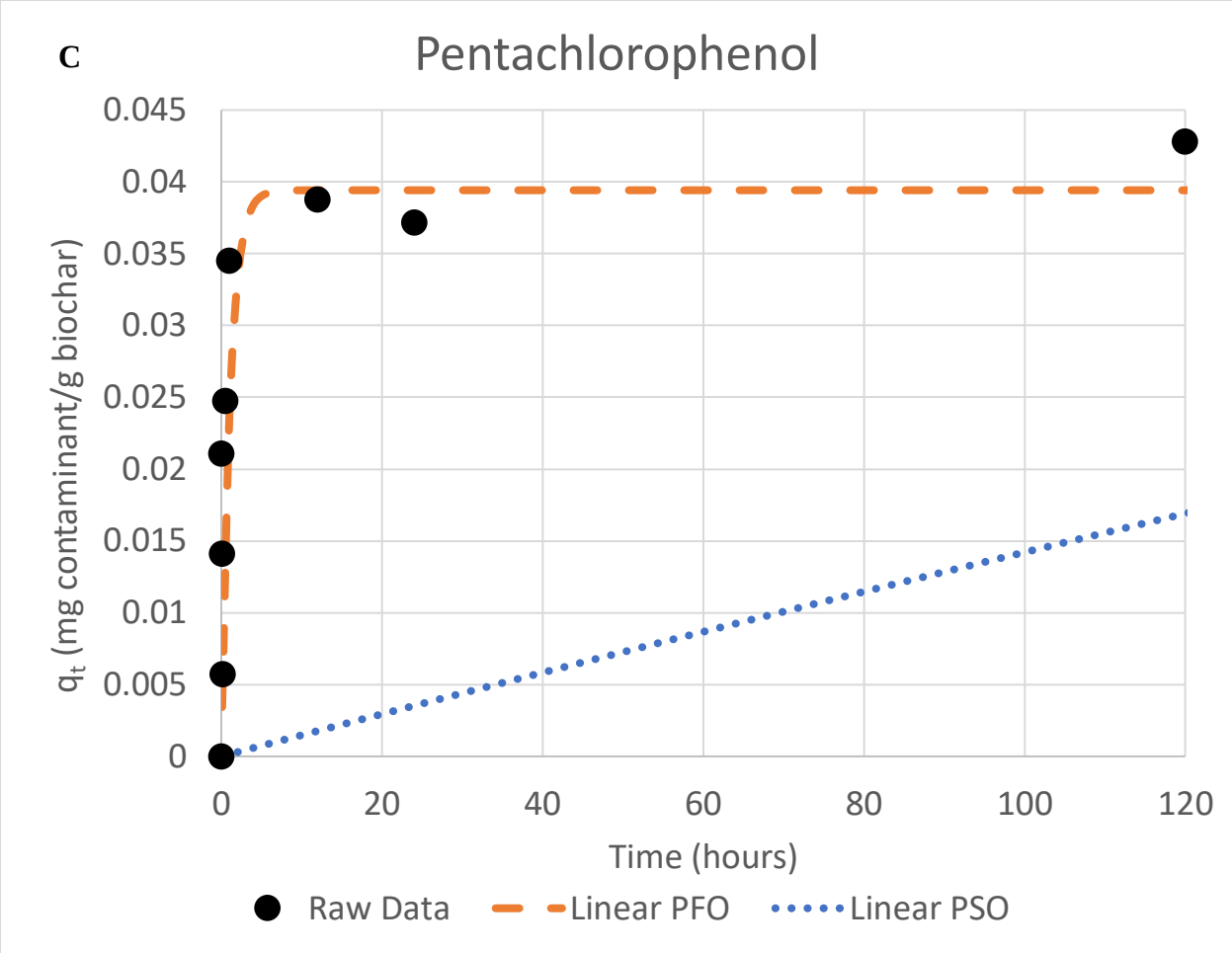

Figure A3 Batch kinetics sorption results of 1 g/L SCG KOH50 µg/L of **A.** diuron, **B.** fipronil and **C.** pentachlorophenol in the SSM in the presence of 10 mg-C/L NOM. Fits were performed using linear pseudo first order and pseudo second order models.